

 Open access • Posted Content • DOI:10.1101/247999

Genetic potential for disease resistance in a critically endangered frog decimated by chytridiomycosis — Source link

Tiffany A. Kosch, Catarina N. S. Silva, Laura A. Brannelly, Alexandra A. Roberts ...+3 more authors

Institutions: James Cook University, University of Pittsburgh, Graduate University for Advanced Studies

Published on: 18 Jan 2018 - bioRxiv (Cold Spring Harbor Laboratory)

Topics: Chytridiomycosis, Genetic diversity, Population and Genetic structure

Related papers:

- [Evolutionary & ecological genetics of African wild dogs](#)
- [Whole exome sequencing identifies the potential for genetic rescue in iconic and critically endangered Panamanian harlequin frogs.](#)
- [Long-Term Habitat Fragmentation Is Associated With Reduced MHC IIB Diversity and Increased Infections in Amphibian Hosts](#)
- [Surviving despite reduce MHC variation: selection patterns and genetic variation of the endangered Huillín \(Lontra provocax\)](#)
- [Genetic signature of disease epizootic and reintroduction history in an endangered carnivore](#)

Share this paper:    

View more about this paper here: <https://typeset.io/papers/genetic-potential-for-disease-resistance-in-a-critically-2sed8d5op1>

1 **Genetic potential for disease resistance in a critically endangered frog decimated by**
2 **chytridiomycosis**

3 Tiffany A. Kosch¹, Catarina N. S. Silva², Laura A. Brannelly^{1,3}, Alexandra A. Roberts¹, Quintin Lau⁴, Lee
4 Berger¹, and Lee F. Skerratt¹

5

6 ¹One Health Research Group, College of Public Health, Medical and Veterinary Sciences, James Cook
7 University, Townsville, Queensland, 4811, Australia

8 ²Centre for Sustainable Tropical Fisheries and Aquaculture, College of Science and Engineering,
9 James Cook University, Townsville, Queensland, 4811, Australia

10 ³Department of Biological Sciences, University of Pittsburgh, Fifth and Ruskin Aves, Pittsburgh, PA,
11 15260, USA

12 ⁴Department of Evolutionary Studies of Biosystems, Sokendai (The Graduate University for Advanced
13 Studies), Kamiyamaguchi 1560-35, Hayama, Kanagawa 240-0193, Japan

14

15 **Keywords:** Major histocompatibility complex, *Pseudophryne corroboree*, *Batrachochytrium*
16 *dendrobatidis*, genetic association, immunogenetics, amphibian declines

17

18 **Corresponding author:** Tiffany Kosch, One Health Research Group, College of Public Health, Medical
19 and Veterinary Sciences, James Cook University, Townsville, Queensland, 4811, Australia, fax: +061
20 07-4725-5659, email: tiffany.kosch@gmail.com

21

22 **Running title:** Corroboree frog conservation genomics

23 **Abstract**

24 Southern corroboree frogs (*Pseudophryne corroboree*) have been driven to functional extinction in
25 the wild after the emergence of the amphibian fungal pathogen *Batrachochytrium dendrobatidis*
26 (*Bd*) in southeastern Australia in the 1980s. This species is currently maintained in a captive
27 assurance colony and is managed to preserve the genetic diversity of the founding populations.
28 However, it is unlikely that self-sustaining wild populations can be re-established unless *Bd*
29 resistance increases. We performed a *Bd*-challenge study to investigate the association between
30 genetic variants of the major histocompatibility complex class IA (MHC) and genome-wide single
31 nucleotide polymorphisms (SNPs). We also investigated differences in *Bd* susceptibility among
32 individuals and populations, and the genetic diversity and population genetic structure of four
33 natural *P. corroboree* populations. We found several MHC alleles and SNPs associated with *Bd*
34 infection load and survival, provide evidence of significant structure among populations, and
35 identified population-level differences in the frequency of influential variants. We also detected
36 evidence of positive selection acting on the MHC and a subset of SNPs as well as evidence of high
37 genetic diversity in *P. corroboree* populations. We suggest that low interbreeding rates may have
38 contributed to the demise of this species by limiting the spread of *Bd* resistance genes. However, our
39 findings demonstrate that despite dramatic declines there is potential to restore high levels of
40 genetic diversity in *P. corroboree*. Additionally, we show that there are immunogenetic differences
41 among captive southern corroboree frogs, which could be manipulated to increase disease
42 resistance and mitigate the key threatening process, chytridiomycosis.

43

44 **1 | INTRODUCTION**

45 Southern corroboree frogs (*Pseudophryne corroboree*) are one of the world's most threatened
46 vertebrate species, with fewer than 50 individuals remaining in the wild (Hunter *et al.* 2010a;
47 McFadden *et al.* 2013). This species has been driven to functional extinction after the emergence of

48 the amphibian fungal pathogen *Batrachochytrium dendrobatidis* (*Bd*) in southeastern Australia in the
49 1980's (Hunter *et al.* 2010b). *Bd* is known to infect at least 500 species of amphibians (Olson *et al.*
50 2013) and has caused dramatic declines and extinctions in the Americas and Australia (Berger *et al.*
51 1998; James *et al.* 2015). In Australia, *Bd* was first detected in Brisbane in 1978 and subsequently
52 spread northwards and southwards along the east coast driving six species to extinction and at least
53 seven others to near extinction (Scheele *et al.* 2017; Skerratt *et al.* 2016).

54 *P. corroboree* are dependent on captive assurance colonies for their continued survival. A
55 breeding and reintroduction program (involving ~1000 adult frogs) is also underway to conserve this
56 species in the wild (Hunter 2012; Lees *et al.* 2013). However, low recapture rates of released frogs
57 suggest that they are still succumbing to *Bd* (Hunter *et al.* 2009), as has been observed with
58 reintroduction efforts in other *Bd*-threatened frogs (Brannelly *et al.* 2015b; Garner *et al.* 2016;
59 Hudson *et al.* 2016; McFadden *et al.* 2010). This is a common challenge for reintroduction programs
60 where threats cannot be readily mitigated (e.g., infectious diseases or climate change). Most captive
61 breeding programs aim to maintain genetic diversity and “freeze” the genetic structure of the wild
62 source populations through time (Ballou & Lacy 1995; Schad 2007). They do not allow for adaptation
63 to natural threats to occur and hence, species often remain vulnerable to the threatening processes
64 that caused their declines (Schad 2007; Woodhams *et al.* 2011). Since the ultimate goal of captive
65 breeding efforts is to reestablish self-sustaining wild populations, a better long term approach may
66 be to apply genetic manipulation methods to increase resilience to the threatening process.
67 Techniques such as marker-assisted selection, genomic selection, and transgenesis are well
68 established in livestock, forestry, and crop improvement (Hayes *et al.* 2009; Hebard 2006; Jannink *et*
69 *al.* 2010; Newhouse *et al.* 2014; Petersen 2017; Whitworth *et al.* 2016), but have yet to be applied to
70 wildlife conservation (Scheele *et al.* 2014; Woodhams *et al.* 2011). Recent advances in molecular
71 genetics have enabled the development of methods, such as genotyping-by-sequencing, for non-
72 model species (Narum *et al.* 2013), which may allow genetic manipulation to be applied to wildlife
73 for the first time.

74 Before genetic manipulation methods can be applied, detailed genomic studies must be
75 performed to establish basic information on *Bd* immunity, including measuring phenotypic and
76 genetic variance, and identifying genes associated with *Bd* resistance. The major histocompatibility
77 complex (MHC) gene region has received the most attention in the context of *Bd* immunity, due to
78 its critical role in initiating the adaptive immune response to pathogens in vertebrates. The MHC
79 consists of several different classes of molecules, including MHC class IA that present peptides
80 derived from intracellular pathogens to cytotoxic T cells, and MHC class IIB that present extracellular
81 peptides to helper T cells (Bernatchez & Landry 2003; Janeway et al. 2005). Genetic polymorphism of
82 the MHC peptide binding region (PBR) determines the repertoire of pathogens that individuals and
83 populations can respond to, making it a good candidate marker for disease association studies and
84 population viability estimates (Sommer 2005; Ujvari & Belov 2011).

85 MHC class IIB alleles, conformations, supertypes, and heterozygosity have been associated
86 with *Bd* resistance (Bataille et al. 2015; Savage & Zamudio 2011; Savage & Zamudio 2016). *Bd*
87 resistance is believed to be associated with PBR chemistries that increase the affinity of MHC
88 molecules to bind *Bd* peptides. For example, *Bd*-resistant individuals have a distinct MHC class IIB
89 conformation for the P9 PBR pocket that consists of an aromatic residue at $\beta 37$, Asp $\beta 57$, Pro $\beta 56$,
90 and a hydrophobic $\beta 60$ residue (Bataille et al. 2015). Although several studies have investigated the
91 association between MHC class IIB and *Bd* resistance, the role of MHC class IA has not yet been
92 examined. The intracellular life stages of *Bd* make it a likely target for MHC class IA presentation
93 (Kosch et al. 2017; Richmond et al. 2009). Furthermore, evidence that southern corroboree frogs
94 have high MHC class IA diversity and that selection is acting on this gene region suggests that it may
95 play a role in *Bd* immunity in this species (Kosch *et al.* 2017).

96 Although we know that the MHC is important to *Bd* immunity, very little is known about the
97 contribution of other genes to *Bd* resistance. Evidence from transcriptome and immunological
98 studies suggests that multiple gene regions are involved in *Bd* immunity (e.g., Ellison *et al.* 2014b;

99 Rollins-Smith *et al.* 2009; Rollins-Smith *et al.* 2006). Characterizing the genetic architecture (i.e., how
100 many genes are involved and their effect size) of *Bd* resistance is fundamental to understanding how
101 this trait evolves and for making predictions of the potential for populations to persist in the
102 presence of *Bd*. One commonly used approach to identify the variants controlling phenotypic traits is
103 genome-wide association studies (GWAS), using genome-wide single nucleotide polymorphism (SNP)
104 data (Bush & Moore 2012; Quach & Quintana-Murci 2017). GWAS also allow genetic relatedness
105 between individuals from natural populations to be estimated (i.e., realized genetic relatedness),
106 which circumvents the necessity of pedigree data for estimating heritability (i.e., proportion of
107 phenotypic variation due to genetic variation; h^2) and permits the estimation of SNP effect size that
108 is crucial for characterizing trait genetic architecture (Visscher *et al.* 2017).

109 Population differences in structure and genetic diversity can be also used to investigate the
110 evolutionary potential of endangered species (Harrisson *et al.* 2014). Genetic diversity forms the
111 basis for adaptation and is a major element for species conservation. Unexpectedly large differences
112 of allele frequencies between populations can be indicative of natural selection (Lewontin &
113 Krakauer 1973). Genome-wide selection scans (GWSS) allow the detection of regions putatively
114 under selection by identifying markers excessively related with population structure and therefore,
115 potential candidates for local adaptation (i.e., outlier markers; Luu *et al.* 2017; Oleksyk *et al.* 2010).
116 Although GWSS methods are currently limited in their ability to detect polygenic traits under
117 selection (Harrisson *et al.* 2014), a combination of approaches may detect subtle phenotype-
118 genotype associations and changes in allele frequencies, which may shed light into the processes
119 driving the evolution of *Bd* resistance.

120 The ability of natural populations to evolve disease resistance by directional selection is a
121 key component to conserving species threatened by emerging infectious diseases. This process is
122 dependent upon two factors: 1) the presence of phenotypic variation that differentially impacts
123 survival or reproductive success, and 2) the existence of additive genetic variation for disease

124 resistance (i.e., heritability; Allendorf *et al.* 2013). Here, we aimed to assess how genetic factors
125 explain differences in *Bd* susceptibility in natural populations of southern corroboree frogs. We
126 tested the following hypotheses using frogs experimentally exposed to *Bd*: (i) survival varies across
127 infected individuals and populations; (ii) genetic variation at MHC loci and/or SNPs associates with
128 infection load and survival; and (iii) MHC alleles and/or SNPs associated with survival show
129 signatures of selection. Our approach is novel from that of previous studies in that this is the first
130 genetic association study to investigate the association between chytridiomycosis resistance and
131 MHC class IA, and the first to use a genome-wide approach to characterize the genetic architecture
132 of this trait. Since our ultimate goal is to improve the success of the *P. corroboree* captive breeding
133 program, we also analyzed the genetic structure and diversity of four of the founder populations of
134 the captive assurance colony. We characterized their evolutionary potential and made
135 recommendations on future research to improve the resistance of this species to *Bd*.

136 **2 | MATERIALS AND METHODS**

137 **2.1 | ANIMAL HUSBANDRY**

138 This study used *P. corroboree* (n=76) that were excess to the captive breeding program, and donated
139 by the Amphibian Research Centre (Victoria, Australia). Frogs were collected as eggs from the wild
140 from four separate populations (Cool Plains-C (n = 20), Jagumba-J (n = 18), Manjar-M (n = 22),
141 Snakey Plains-S (n = 16)); approximate distances between populations ranged from 6 to 19 km
142 (mean=12 km \pm 5.25 SD) (for site map see Kosch *et al.* 2017; Fig 1) and raised in disease free
143 conditions until the start of our experiment. Frogs were housed individually in 300 x 195 x 205 mm
144 terraria with a damp and crumpled paper towel substrate (Earthcare®, ABC Tissue) at 18-20°C, and
145 were fed *ad libitum* three times weekly with 5 – 10 mm crickets (*Acheta domestica*). They were
146 misted twice daily for 60 s with reverse osmosis water, and temperature and humidity were
147 monitored daily. Terraria were cleaned fortnightly by replacing the paper towel. The animals used in

148 this experiment were part of a larger study (e.g., Brannelly *et al.* 2016b; Kosch *et al.* 2017). Animal
149 ethics approval was granted by James Cook University for this study under application A1875.

150 **2.2 | EXPERIMENTAL *Bd* EXPOSURES**

151 Corroboree frogs were allowed to acclimatize to their new environment for 7 d before the start of
152 the experiment, when they were inoculated with a New South Wales strain of *Bd* (AbercrombieR-
153 L.booroologenesis-2009-LB1 passage number 11)(*Bd* treatment, n=76; controls, n=17). *Bd* zoospores
154 were harvested from flooded TGhL petri plates and quantified using a haemocytometer. Animals
155 were inoculated with 1×10^6 zoospores by applying 3 mL of inoculum onto the venter. Animals were
156 then placed in individual 40 mL containers for 6 h, and then returned to their individual terraria. *Bd*
157 negative control animals were mock-inoculated using *Bd* negative TGhL petri plates (n = 17). We
158 measured *Bd* infection load weekly until the end of the experiment (n = 103 d) by quantitative
159 polymerase chain reaction (qPCR) analysis of skin swabs (Boyle *et al.* 2004) using the swabbing
160 protocol and DNA extraction methods previously described (Brannelly *et al.* 2015a). Each qPCR
161 analysis contained a positive and negative control, a singlicate series of dilution standards, and one
162 replicate of each sample (Kriger *et al.* 2006; Skerratt *et al.* 2011). We monitored body condition
163 throughout the experiment by measuring mass (to the nearest 0.01 g) and snout to vent length (SVL)
164 weekly. Body condition was estimated by $\text{Log}_{10}(\text{Mass}+1)/\text{Log}_{10}(\text{SLV}+1)$. Frogs were checked daily
165 for general health and clinical signs of chytridiomycosis (Brannelly *et al.* 2015c) and were euthanized
166 with an overdose of MS-222 in accordance with animal ethics guidelines if deemed moribund. Any
167 animals that cleared infection and survived until the end of the experiment were returned to the
168 Amphibian Research Centre.

169 Survival data between populations was analysed by Cox Regression analysis using the
170 survival package in R (Therneau 2015; Therneau & Grambsch 2000). Infection loads were
171 transformed by taking the Log_{10} of zoospore equivalents (ZE) + 1, and analysed using mixed models
172 with nlme in R (Pinheiro *et al.* 2009). Constructed models included the explanatory (fixed) factors of

173 week, population, week*population, and days survived. ANOVA was used to evaluate which models
174 best fit the data.

175 **2.3 | MHC CLASS I GENOTYPING**

176 *DNA extraction and PCR.* DNA was extracted from various tissues (skin, muscle, kidney, toe clips)
177 using an ISOLATE II Genomic DNA Kit (Bioline) following the manufacturer's instructions. DNA
178 concentration and quality was measured with a Nanodrop2000 (Thermo Fisher), and extracts were
179 stored at -20°C until use. Polymerase chain reaction (PCR) amplification was performed using *P.*
180 *corroboree* MHC class IA exon 2 primers (PcIAex2-2F1, PcIAex2-2R1), which amplify the
181 hypervariable α 1 peptide binding region (PBR) domain (Kosch *et al.* 2017). Initially, PCRs were
182 performed with *Taq* DNA polymerase, but preliminary sequencing runs suggested that the DNA
183 polymerase and reaction conditions were leading to sequencing errors (indicated by the occurrence
184 of single bp changes not replicated across multiple sequences). Therefore we modified PCR
185 conditions to minimize PCR errors and artefact formation for the remaining runs using previously
186 described modifications (Babik 2010; Judo *et al.* 1998; Zylstra *et al.* 1998). Specifically, we switched
187 to a high fidelity DNA polymerase (NEB Q5 High-Fidelity PCR Kit), decreased DNA template amount
188 to 60 ng, increased annealing temperature to 67°C, increased elongation time to 3 min, and reduced
189 cycle number to 25 (see Methods S2 for complete reaction details).

190 Resulting PCR products were separated by gel electrophoresis and bands of the correct size
191 were excised and extracted with a FavorPrep Gel Purification Kit (Favorgen) following the bench
192 protocol. PCR bands generated using the Q5 PCR kit were extracted with a different kit (NEB
193 Monarch PCR & DNA Cleanup Kit) to inactivate the exonuclease included in the reaction and A-tailed
194 before ligation (see Methods S2 for A-tailing reaction).

195 *Cloning and sequencing.* All PCR products were ligated with a pGEM®-T Easy Vector kit (Promega),
196 and recombinant DNA was transformed into Top 10 competent *Escherichia coli*. Cells were grown on
197 LB agar plates (with 100 μ g/ml ampicillin and 20 μ g/ml X-Gal) for 16 h at 37°C. We used blue-white

198 screening to select 16 to 24 clones from each transformation and amplified them with SapphireAmp
199 Fast PCR Master Mix (Takara) and M13 primers. Multiple independent PCRs were run for a
200 proportion (n = 32) of the individuals to rule out single copy alleles and potential PCR artefacts
201 (Table S1). We also used previously published sequence data available for a subset of the individuals
202 (Kosch *et al.* 2017) to confirm genotypes.

203 PCR products were purified for sequencing by a clean-up reaction of 10 µl of PCR product, 1
204 U of Antarctic phosphatase (NEB), 1 U of exonuclease (NEB), and 2.6 µl of RNase-free water and the
205 thermal cycler program: 37°C for 30 min, 80°C for 20 min, and 4°C for 5 min. Resulting purified PCR
206 products were then shipped to Macrogen (Seoul, South Korea) for unidirectional Sanger sequencing.
207 *MHC sequence analysis.* Resulting sequences were analyzed with Geneious (v. 9.0.5) and identified
208 as alleles if: (i) BLAST results indicated they were MHC Class IA sequences, (ii) they did not include
209 stop codons, and (iii) they were present in more than one copy per individual and more than one
210 independent PCR reaction. Alleles were named based upon MHC nomenclature rules described in
211 Klein *et al.* (1993), and were assigned to supertypes to explore functional diversity. Supertype
212 designation was performed by first aligning corroboree frog amino acid sequences with that of
213 *Homo sapiens* (HLA-A; D32129.1). Next we extracted amino acid sequences from the 13 PBR pocket
214 positions identified in previous studies (Lebrón *et al.* 1998; Matsumura *et al.* 1992) using R. We then
215 characterized the 13 sites for five physiochemical descriptor variables: z1 (hydrophobicity), z2 (steric
216 bulk), z3 (polarity), z4 and z5 (electronic effects) (Didinger *et al.* 2017; Sandberg *et al.* 1998) and
217 performed discriminant analysis of principle components (DAPC) with R package adegenet (Jombart
218 *et al.* 2010) to define functional genetic clusters. Alleles were assigned to clusters by a K-means
219 clustering algorithm by selecting the model with the lowest Bayesian information criterion (BIC).

220 We tested for recombination in our nucleotide alignment with the genetic algorithm
221 recombination detection (GARD) method executed on the Datamonkey server (Delpont *et al.* 2010;
222 Kosakovsky Pond *et al.* 2006). In MEGA7, we tested for evidence of positive selection with the Z-test

223 of selection on three datasets: (i) the entire MHC class IA alignment, (ii) putative PBR pockets, and
224 (iii) non-putative PBR pocket nucleotides using the modified Nei-Gojobori method (Jukes-Cantor)
225 and 500 bootstrap replications (Kumar *et al.* 2016; Nei & Gojobori 1986). Positive selection at the
226 codon level (dN/dS or $\omega > 1$ with a posterior probability of > 0.95) was estimated with omegaMap (v
227 5.0) (Wilson & McVean 2006) following similar conditions to (Lau *et al.* 2016). Tajima's D test of
228 neutrality was executed in MEGA7. Evolutionary relationships among *P. corroboree* nucleotide
229 sequences and other vertebrates were inferred by constructing Neighbor-Joining (NJ) phylogenetic
230 trees in MEGA7. Evolutionary distances were computed using the Kimura 2-parameter gamma
231 distributed method (K2+G) and tree node support was estimated via 500 bootstrap replicates
232 (Felsenstein 1985).

233 We investigated population differences in MHC class IA diversity using five measures: (i) the
234 number of unique alleles per population (A_P); (ii) the number of alleles per individual (A_I); (iii) mean
235 evolutionary distance between nucleotide (D_{NUC}) and amino acid (D_{AA}) variants estimated with
236 MEGA7 (Kumar *et al.* 2016) as the number of differences over all sequence pairs within each
237 individual using a p-distance model; (iv) the total number of MHC supertypes per population (S_P);
238 and (v) the mean number of MHC supertypes per individual by population (S_I). Number of alleles (A_I)
239 and supertypes (S_I) per individual were summarized with a generalized linear model (GLM) in R
240 assuming a Poisson distribution to model the count data. One-way analysis of variance (ANOVA) in R
241 was used to compare population evolutionary distances between nucleotides (D_{NUC}) and amino acids
242 (D_{AA}). Arlequin was used to estimate pairwise fixation index (F_{ST}), population differentiation based on
243 variance of allele frequencies among populations (Excoffier & Lischer 2010). The theoretical range of
244 F_{ST} values is from 0 to 1, with 0 indicating complete panmixia and 1 indicating two isolated
245 populations.

246 **2.4 | SNP GENOTYPING AND QUALITY CONTROL**

247 To investigate the genome-wide association with infection load and survival, all infected individuals
248 ($n = 76$) were genotyped by Diversity Arrays Technology Sequencing (DARTseq, Canberra, Australia).
249 This method uses hybridization-based sequencing technology implemented on an NGS platform to
250 identify thousands of single nucleotide polymorphisms (SNPs) in one reaction (Cruz *et al.* 2013).
251 Because high molecular weight DNA is necessary for DARTseq analysis, we examined our DNA
252 samples by gel electrophoresis before shipping. A subset of samples from extracted skin ($n = 23$),
253 were re-extracted from kidney tissue due to the presence of extensive nucleosome ladders or
254 smearing. Samples were then diluted to 50 ng/ μ l with TE Buffer to a final volume of 15 μ l for
255 DARTseq analysis.

256 Sequence read quality was filtered for >10 Phred quality score and minimum pass
257 percentage of 50. Initial SNP quality control was performed by DARTdb with >3 reads per SNP and
258 $>95\%$ reproducibility. Further filtering (MAF of 2%, call rate 70%, duplicate removal) and data
259 formatting was then performed with dartQC (<https://github.com/esteinig/dartQC>) resulting in 3,489
260 SNPs.

261 **2.5 | GENOTYPE-PHENOTYPE ASSOCIATION ANALYSIS**

262 *Genome-wide association analyses.* We applied more stringent quality control with the GenABEL
263 'check.marker' function to exclude SNPs with a call rate $\leq 95\%$ and individual call rate $\leq 95\%$
264 (Aulchenko *et al.* 2007). We also excluded two individuals in which the identity by state (IBS) was
265 greater than 0.9. We evaluated Hardy–Weinberg equilibrium (HWE) independently for each
266 population and removed SNPs if they failed this test ($P \leq 0.001$) in all four populations. After quality
267 control, 3,245 SNPs remained for GWAS analysis. To investigate the associations between SNPs and
268 the phenotypic traits we ran a separate GWAS for each phenotypic trait, three in total: (i) maximum
269 infection load (log transformed), (ii) days survived (log transformed), and (iii) infection load per
270 week. Maximum infection load and days survived were tested using mixed models in the R package

271 GeneABEL (Aulchenko et al. 2007). Repeated measurements of infection load per week were rank
272 transformed using the 'rntransform' function in GenABEL and analysed using the function 'rGLS' in
273 the R package RepeatABEL (Rönnegård et al. 2016). We accounted for the effects of size in models (i)
274 and (iii), sex in model (ii) and week in model (iii), as these factors were significantly associated with
275 the trait. To account for multiple hypothesis testing, the p-value significance thresholds were
276 adjusted with the Bonferonni equation using two different alpha thresholds (alpha=0.05, significant;
277 alpha=1.0, suggestive) (Clarke et al. 2011). The heritability values (h^2_{SNP}) of each of the ten SNPs with
278 the smallest P-values (i.e., top 10 SNPs) were estimated as V_{SNP}/V_P (V_P is the phenotypic variance
279 estimate for the phenotypic trait and $V_{SNP}=2pqa^2$, where p and q are the frequencies of the major
280 and minor allele frequencies, respectively, and a is the additive SNP effect (Falconer et al. 1996). The
281 top ten SNPs from each of the three GWAS were annotated by searching the NCBI non-redundant
282 nucleotide database with the software package Blast2GO (Götz et al. 2008).

283 **2.6 | POPULATION GENETIC ANALYSES**

284 Several measures were used to estimate population genetic variation and thus assess long-term
285 evolutionary potential of *P. corroboree* populations. Mean allelic richness (A_R) was estimated using
286 the R package PopGenReport (Adamack & Gruber 2014). Observed heterozygosity (H_O), expected
287 heterozygosity (H_E) and inbreeding coefficient (F_{IS}) were estimated using the R package diversity
288 (Keenan *et al.* 2013). Effective population size (N_e) was estimated using the software NeEstimator v.2
289 using the linkage disequilibrium method and a random mating model (Do *et al.* 2014). Expected
290 heterozygosity (H_E) is the best overall estimate of genetic variation, and can be compared to H_O to
291 estimate inbreeding rates (i.e., $H_E > H_O$ suggests excessive inbreeding) (Allendorf *et al.* 2013). Allelic
292 richness (A_R) measures allelic diversity while considering sample size. This method is more likely to
293 detect population bottlenecks than H_E (Allendorf 1986). Effective population size (N_e) indicates the
294 rate of heterozygosity loss over time due to stochastic factors such as genetic drift (i.e., populations
295 with smaller N_e have a greater rate of heterozygosity loss through time) (Allendorf *et al.* 2013;
296 Kliman *et al.* 2008).

297 Pairwise F_{ST} values were calculated using the software GenePop on the web (Rousset 2008).
298 An exact G-test was also calculated in GenePop (Markov- chain parameters: 10,000 dememorisation
299 steps, 1000 batches and 10,000 iterations per batch) for each population pair using the G log
300 likelihood ratio.

301 Outlier markers were identified using the PCAdapt R package (Luu *et al.* 2017) with $K = 9$ and
302 $\text{min.maf} = 0.01$. The candidate loci were determined using Benjamini–Hochberg FDR (false discovery
303 rate) control and the level of FDR was set to 0.01. To evaluate the genetic relationships among
304 individuals, discriminate analysis of principal components (DAPC) was performed using adegenet
305 package in R (Jombart 2008) for neutral and outlier SNPs. The a -score approach was used to assess
306 the stability of the DAPC analyses (i.e. trade-off between power of discrimination and over-fitting).
307 Across all 100 permutations the highest a -score was 0.655 for 3 PCs.

308 **2.7 | POPULATION STRUCTURE BASED ON MHC CLASS IA AND SNP DATA**

309 We used the program STRUCTURE 2.3.4 (Pritchard *et al.* 2000) to examine clustering of source *P.*
310 *corroboree* populations based on either MHC class IA or SNP genotypes. For MHC class IA, because
311 multiple MHC loci were amplified, we entered data recessive alleles based on the approach used for
312 AFLP data sets (Falush *et al.* 2007). The four populations were incorporated into the admixture
313 model. We determined the number of genetic clusters of individuals (K) using the method of Evanno
314 *et al.* (2005) to calculate ΔK in STRUCTURE HARVESTER (Earl 2012). We tested a range of $K = 1$ to
315 $K = 5$ with 10 replicates of each K , using 100,000 iterations following a burn-in period of 100,000
316 iterations.

317 **3 | RESULTS**

318 **3.1 | SURVIVAL AND INFECTION LOAD OVER TIME**

319 *Survival.* Five frogs in the *Bd*-inoculated group survived to the end of the experiment, four of which
320 were from population M (18.2%), and one from population C (5.0%). All animals in the negative
321 control group survived the experiment. Frogs became ill and were euthanized between day 21 and

322 day 94 post inoculation. Cox proportional hazards regression indicated that population of origin had
323 a significant impact on days survived (Figure 1) (Cox regression: $\chi^2_3 = 9.72$, $P < 0.05$), with population
324 M surviving on average 14.2 days longer than the other three populations.

325

326 *Infection load.* All *Bd*-inoculated frogs were *Bd* positive for at least two weeks during the experiment,
327 and infection loads increased over time in all but the 5 survivors. Negative controls remained *Bd*-
328 negative throughout the duration of the experiment. Body condition during the experiment
329 decreased in *Bd* inoculated frogs, but not controls (Figure S1). Four frogs (5.3%; population M, $n = 3$;
330 population C, $n = 1$) successfully cleared infection by week 12. The fifth survivor had a low infection
331 load (6.7 ZE) at the end of the experiment and later cleared infection naturally. The overall log of
332 infection load increased dramatically in the first half of the experiment (slope = 0.835), and then
333 plateaued in the second half (slope = -0.225) (Figure 1). To account for this change of slope through
334 time, the dataset was subdivided into two datasets (early < 5.5 weeks and late > 5.5 weeks) before
335 mixed effects modelling. ANOVA results comparing models of infection load indicated that the model
336 of best fit for both early and late datasets included days survived (transformed with a quadratic
337 function to improve linearity), allowed infection load to vary by population, had a Week*Population
338 interaction factor, and included individual ID as a random effect (ANOVA, AIC = 1066, $\chi^2_{215} = 7.321$, P
339 = 0.062; AIC = 456, $\chi^2_{15} = 21.260$, $P < 0.0001$). Infection load did not differ between populations in
340 either the early or late dataset (Mixed models, $F_{3,47} = 0.507$, $P = 0.678$; $F_{3,54} = 1.540$, $P = 0.215$), but
341 there was a significant interaction of Population*Week in the late dataset (Mixed models, $F_{3,124} =$
342 3.156, $P < 0.05$) with population M having a significantly different slope than the other 3 populations
343 (ANOVA, $F_{3,185} = 14.63$, $P < 0.001$). The change in the slope of population M in the late dataset was
344 due to the impact of the 4 surviving individuals reducing infection from moderate levels, rather than
345 individuals recovering from high infection burdens.

346 3.2 | MHC DIVERSITY AND EVOLUTION

347 *MHC allele diversity.* We identified a total of 22 MHC class IA alleles, with a range of 2 to 10 alleles
348 per individual (Table S2). Alleles blasted with high similarity to MHC IA sequences from *P. corroboree*
349 (KX372222-KX372242, and KY072979-KY072985), *Rana clamitans* (JQ679356), and *R. temporaria*
350 (FJ385608) (Kiemnec-Tyburczy *et al.* 2012; Kosch *et al.* 2017; Teacher *et al.* 2009). There were no
351 differences in number of alleles per individual (A_i) (GLM, $X^2 = 3.852$, d.f. = 3, $P = 0.278$), mean
352 evolutionary distance between nucleotide variants (D_{NUC}) (GLS, $F_{3,71} = 2.527$, $P = 0.0643$), and mean
353 evolutionary distance between amino acid variants (D_{AA}) (GLS, $F_{3,71} = 1.877$, $P = 0.141$) among
354 populations (Table 1, Figure S5). The most common MHC allele, Psco-UA*9, was present in > 70% of
355 individuals across populations (range = 31.0% – 85.0%) (Table S3, Figure 3b). Alleles Psco-UA*24 and
356 Psco-UA*27 were unique to population C and alleles Psco-UA*18 and Psco-UA*19 were unique to
357 population M. F_{ST} values of the MHC class IA were significant at $p < 0.05$ level for three of six pairwise
358 comparisons involving the four populations (M x C, M x J, M x S; range: 0.000 – 0.012; Table 2).

359

360 *MHC evolution.* We found no evidence of recombination between MHC alleles. There was evidence
361 of positive selection acting on codons of the putative PBR pocket sites ($dN/dS = 2.128$, $Z = 2.921$, $P <$
362 0.01), but no evidence of positive selection on the non-PBR pocket sites ($dN/dS = 0.590$, $Z = -1.702$, P
363 $= 1.000$) or the entire MHC Class IA region ($dN/dS = 0.693$, $Z = -0.027$, $P = 1.000$). Tajima's D value of
364 > 0 on the entire alignment indicates that balancing selection or sudden population contraction has
365 occurred ($D = 1.09$). In total, omegaMap identified 11 codons with evidence of positive selection, of
366 which 7 sites aligned with codons of HLA-A PBR pocket positions (Figures 2 and S3; 1, 16, 26, 53, 56,
367 57 and 60). Three of these sites (16, 56, and 57) have been previously identified as being under
368 positive selection in this species (Kosch *et al.* 2017).

369

370 *MHC supertype diversity.* Conversion of 22 MHC alleles into functional superotypes resulted in 8
371 distinct superotypes, with each supertype containing one to four alleles (Figure S3). The most
372 common MHC supertype, ST8, was present in > 80% of individuals (range = 68.0% – 90.0%) (Table S4,
373 Figure 3a). MHC superotypes corresponded to groups of clades within the NJ phylogeny (Figure S4).
374 Superotypes 1 and 2 were each comprised of a single allele. Superotypes 4 and 5 formed two distinct
375 clades, while superotypes 3, 6, 7, and 8 were split into separate clades dispersed throughout the
376 phylogeny. The number of superotypes per individual (S_i) ranged from 1 to 8 (mean = 4.83 ± 1.53 SD)
377 with no difference among populations (GLM, $X^2 = 2.16$, d.f. = 3, $P = 0.541$).

378 **3.3 | ASSOCIATION ANALYSIS**

379 *MHC association.* Alleles Psco-UA*5 and Psco-UA*9 were positively associated with maximum
380 infection load (Table S5; GLS, $F_{1,74} = 4.11$, $P < 0.05$, $F_{1,74} = 10.56$, $P < 0.01$). Allele Psco-UA*23 was
381 negatively associated with number of days survived (Table S6; GLS, $F_{1,74} = 12.96$, $P < 0.001$). Allele
382 Psco-UA*5 was least common in the more resistant population M ($23\% \pm 0.19$) and most common in
383 the susceptible population J ($78\% \pm 0.21$) (Table S3, Figure 3a). Strangely, alleles Psco-UA*9 and
384 Psco-UA*23 were relatively common in the more resistant population M ($77\% \pm 0.19$ and $18\% \pm 0.19$
385 respectively). Individuals with ST8 had higher maximum infection loads than those with other STs
386 (Table S7; GLS, $F_{1,74} = 4.49$, $P < 0.05$) and a greater chance of dying (Figure S6; GLS, $F_{1,73} = 7.29$, $P <$
387 0.01).

388

389 *GWAS.* The association analyses did not identify any significant SNPs after correction for multiple
390 testing (Figures 4 and S7), although one SNP (173) was suggestively negatively associated with days
391 survived ($P=9.2e-05$; Table S9; Fig 4). In general, each one of the top SNPs explained only a small
392 proportion of the phenotypic variation. Two SNPs (1894 and 1895) were identified in the top ten
393 markers positively associated with both maximum infection load (GenABEL) and infection load per
394 week (RepeatABEL). BLAST results revealed that 96% of the top SNPs had sequence homologies with

395 other amphibians, including *Xenopus tropicalis*, *X. laevis*, *Nanorana parkeri*, and *Andrias davidianus*
396 (Table S10). Several of the top SNPs were homologous to genes that are known to impact immunity
397 and included functions such as pathogen recognition and control and immune cell proliferation
398 (Table 4).

399 **3.4 | GENETIC DIVERSITY AND STRUCTURE OF SNPS**

400 PCAdapt analyses with a false discovery rate (FDR < 0.01) resulted in 3465 neutral and 24 outlier
401 SNPs. F_{ST} values from all SNPs ranged from 0.106-0.191, F_{ST} values from neutral SNPs ranged from
402 0.105-0.188 and F_{ST} values from outliers ranged from 0.241-0.601 with populations M and J being
403 the most differentiated and populations S and J being the least differentiated for all datasets (i.e.
404 including all SNPs, neutral and outlier SNPs; Table 2). DAPC plots using neutral SNPs showed all the
405 populations clustering independently. When using only the 24 outlier SNPs, population M was
406 distinctively separated from the remaining populations (Figure 5).

407 Allelic richness values (A_R) ranged from 1.34 in populations J and S to 1.38 in population M.
408 Observed heterozygosity (H_O) values ranged from 0.361 in population S to 0.401 in population M,
409 and were higher than expected heterozygosity (H_E) in all populations suggestive of low inbreeding
410 rates. Inbreeding coefficients (F_{IS}) were negative in all populations indicating more heterozygous
411 individuals than expected (Table 3). Effective population size values (N_e) were lowest for populations
412 M and C (6.8 and 7.9, respectively; Table 3).

413 **3.5 | COMPARISON OF POPULATION STRUCTURE USING MHC IA AND SNPS**

414 For both MHC class IA and SNP data, STRUCTURE analyses identified an optimum of two clusters ($K=$
415 2), with individuals separating into clusters following similar patterns to fixation index (F_{ST}) results
416 (Table 2, Figure S8). MHC class IA STRUCTURE results indicated that 85% of individuals from
417 population C grouped into one cluster, while only 36.8% individuals from populations M and S
418 grouped into the same cluster. For SNP data, population M is the most divergent from the other
419 three populations, which is in concordance with the DAPC results.

420 **4 | DISCUSSION**

421 Southern corroboree frogs exhibit phenotypic variation in *Bd* susceptibility which is associated with
422 specific MHC class IA alleles and genome-wide SNPs. For example, MHC alleles Psco-UA*5, Psco-
423 UA*9, and Psco-UA*23 were associated with either increased *Bd* infection loads or lower survival
424 times. Multiple SNPs were suggestively correlated with *Bd* resistance including *RALGPS2*, which
425 regulates immune cell proliferation and immunoglobulin Y (*IgY*), an antibody that binds and
426 neutralizes pathogens. Despite dramatic recent declines, *P. corroboree* populations still contain
427 sufficient standing genetic variation from which could be selected for improved survival. For
428 example, detection of positive selection in the MHC class IA region of this species could suggest
429 selection for *Bd* resistance. However, low interbreeding rates among closely interspersed *P.*
430 *corroboree* populations confirm natural history observations for this species of low vagility. This
431 factor explains declines in *P. corroboree* despite evidence for sufficient additive genetic *Bd* resistance
432 in the species. Therefore, *P. corroboree* may benefit from genetic manipulation to improve *Bd*
433 resistance in order to overcome natural history constraints that prevent optimal selection
434 conditions.

435 **4.1 | PHENOTYPIC DIFFERENCES AMONG POPULATIONS**

436 *P. corroboree* exhibit phenotypic variation in resistance to *Bd* infection at the population level. This
437 was evident in both the days survived and infection load through time (Figure 1). One population
438 (M) was distinct from the other three populations by having the longest survival, lowest infection
439 loads, and greatest amount of individuals that survived until the end of the experiment.

440 **4.2 | GENOTYPE-PHENOTYPE ASSOCIATIONS**

441 Phenotypic differences in *Bd* resistance were associated with genetic variance of the MHC and
442 genome-wide SNPs. Three MHC alleles were associated with increased *Bd* susceptibility in individual
443 frogs. Of these, Psco-UA*5 was least common in the more *Bd* resistant M population. MHC
444 supertypes were not associated with resistance, however, supertype ST8 was associated with

445 increased susceptibility. Although this supertype was relatively common, it was more common in the
446 frogs that died (86%) than in survivors (40%), and least common in the more resistant population M
447 (Table S4, Figure 3a).

448 Our GWAS did not identify any SNPs that were significantly associated with *Bd* resistance,
449 which may be the result of the limited sample size available for this study combined with the
450 potential polygenic nature of the traits analyzed here. One SNP (173) was suggestively negatively
451 associated with days survived (Figure 4). This SNP has closest homology to the *RALGPS2* gene of *X.*
452 *tropicalis* that encodes a guanine nucleotide exchange factor (GEF) for the GTPase RALA (Tables 4
453 and S2). These molecular switches are involved in multiple cell processes such as cell differentiation
454 and proliferation (Alberts *et al.* 2002) and may potentially influence *Bd* immunity by regulating
455 epidermal or immune cell proliferation, which are important predictors of *Bd*-related mortality
456 (Ellison *et al.* 2014a). Several of the top 10 SNPs associated with maximum infection load (e.g., 1894,
457 1895) have sequence homology to an alpha-L-tissue fucosidase (*FUCA1*). This enzyme cleaves fucose
458 containing glycoproteins, and is involved in the immunoregulation of leukocyte migration during
459 inflammation (Ali *et al.* 2008). Significantly, poor immune cell recruitment is observed in the skin of
460 *Bd*-infected frogs, due to pathogen-produced immunosuppressants that cause apoptosis (Fites *et al.*
461 2013). It remains to be seen whether suppression of inflammation in chytridiomycosis involves
462 immunoregulation via fucosidases, although preliminary support indicates the increased
463 transcription of fucose binding lectin in frogs after exposure to *Bd* (Ribas *et al.* 2009). A SNP with
464 homology to immunoglobulin Y (IgY) was also identified as a top SNP in this study (3440). IgY is
465 functionally analogous to mammalian IgG, which is essential for pathogen recognition and control
466 (Warr *et al.* 1995). The contribution of IgY to *Bd* immunity varies across species. *Xenopus laevis*
467 immunized against *Bd* produced a strong pathogen-specific IgY response (Ramsey *et al.* 2010),
468 whereas IgY response was suppressed or unaffected in other species (Fernández-Loras *et al.* 2017;
469 Poorten *et al.* 2016; Young *et al.* 2014).

470 **4.3 | GWAS LIMITATIONS**

471 Although GWAS is a powerful tool for detecting SNP-phenotype associations, this method is limited
472 in its ability to detect SNPs with low to moderate effect sizes (Harrisson *et al.* 2014). For example,
473 Barson *et al.* (2015) was successful at identifying a large effect locus controlling age of maturity in
474 Atlantic salmon, but other studies have failed to detect significant loci (e.g., Santure *et al.* 2015). In
475 many cases where significant variants have been associated with phenotypic traits, they only explain
476 a relatively small proportion of the variance (e.g., Bérénos *et al.* 2015; Silva *et al.* 2017). This
477 suggests a quantitative genetic architecture, and that causal loci are being overlooked due to a lack
478 of power to detect multiple small effects (Maher 2008; Yang *et al.* 2010).

479 Therefore, GWAS performs best with large sample sizes and high SNP coverage (Visscher *et*
480 *al.* 2017), making GWAS investigations of threatened or non-model species challenging. For *P.*
481 *corroboree*, power calculations based on the average predicted genomic relationships from the
482 individuals used in this study indicate that to achieve 99.7% power, a sample size of ($n = 1000$) is
483 required if narrow sense heritability of *Bd* resistance is (h^2) > 0 (see Methods S2 for description of
484 power calculations). Future studies with *P. corroboree* should increase the sample size in order to
485 improve GWAS power.

486 **4.4 | POPULATION GENETIC STRUCTURE**

487 Southern corroboree frog populations showed significant evidence of genetic structure between all
488 four populations studied, with population M being the most differentiated in pairwise comparisons
489 across all datasets, and populations J and S the least differentiated (Table 2, Figures 5 and S8). The
490 population divergence estimates for this species are consistent with the life history information (i.e.,
491 high site fidelity, low vagility; Hunter 2000), and microsatellite data indicates that interbreeding
492 among populations separated by even a few km is low (Morgan *et al.* 2008). These factors have likely
493 contributed to the demise of *P. corroboree* after the introduction of *Bd*, despite evidence of *Bd*

494 resistance within some individuals. This is because *Bd* resistance genes are unlikely to spread across
495 the landscape due to low interbreeding rates.

496 Populations C and M showed low effective population sizes (N_e), which reflects the recent
497 demographic history of this species in that it went from highly abundant to functionally extinct
498 within the last ~30 years (Hunter *et al.* 2010b; Morgan *et al.* 2008; Osborne *et al.* 1999). Although we
499 observed an excess of heterozygotes (H_o) and low inbreeding rates (F_{IS})—suggestive of a large,
500 diverse population—this may be due to the relatively low sample sizes available for this study and/or
501 the effects of the recent drastic reduction in population size that might not yet have impacted
502 inbreeding estimates.

503 **4.5 | EVOLUTION OF THE MHC CLASS IA AND SNPS**

504 Tests of selection indicate that codons of the putative MHC peptide binding region pockets are
505 under positive selection in *P. corroboree*, suggesting that these amino acid residues provide a
506 survival advantage to *Bd* infected hosts.

507 Even though we did not detect any MHC alleles associated with *Bd* resistance, our evidence
508 that three MHC alleles and one supertype are associated with higher susceptibility supports the
509 hypothesis that *P. corroboree* MHC has a functional role in *Bd* immunity. In other frog species, MHC
510 class IIB alleles and superotypes have been correlated with increased *Bd* resistance (e.g., Bataille *et al.*
511 2015; Savage & Zamudio 2011) likely due to higher binding affinity for *Bd* peptides. This correlation
512 is also probable for MHC class IA, as has been demonstrated in pathogen systems of humans and
513 other species (Aguilar *et al.* 2016; International H. I. V. Controllers Study *et al.* 2010; Koch *et al.* 2007;
514 Madsen & Ujvari 2006). Future investigations should develop locus specific primers or apply next-
515 generation sequencing to improve the confidence level of genotyping (see Galan *et al.* 2010).
516 Another approach would be to knock-in putative *Bd* immunity-associated MHC alleles using gene
517 editing technologies, such as CRISPR-Cas9 (Doudna & Charpentier 2014), and measure gene effects
518 directly via *Bd* challenge experiments.

519 Of the 24 SNPs that were population outliers (Tables 4 and S11), there are several that likely
520 play an important role in *Bd* immunity due to their homology to pathogen response genes in other
521 species. One of the SNPs under positive selection is a *RAD51* homolog (79). In *Xenopus*, this gene is
522 involved in genetic recombination and DNA repair, and is likely involved in meiotic recombination
523 due to high expression levels in testes and ovaries (Maeshima *et al.* 1996). *RAD51* has also been
524 shown to be strongly expressed in newt testes during spermatogenesis (Yamamoto *et al.* 1999), a
525 process that is increased in *Bd*-infected frogs (Brannelly *et al.* 2016a). Interestingly, another SNP
526 identified under selection in our study had homology to an outer dense fiber that maintains the
527 elastic structure of sperm tails (2794), further highlighting the potential role of increased
528 reproductive effort as a response to *Bd* infection.

529 An additional SNP outlier (2603) has homology to Toll-like receptor 7 (TLR7), which is
530 involved in pathogen recognition and activation of innate immunity via production of specific
531 cytokines. In response to the intracellular fungal pathogen *Histoplasma capsulatum*, murine
532 dendritic cells require TLR7 to control fungal growth and activate T cells via interferon- γ (Van
533 Prooyen *et al.* 2016). It is possible that this gene may also be involved in the response of frogs to *Bd*
534 infection. Other relevant SNPs outliers include those that may act in response to *Bd*-induced effects
535 on hematopoietic tissue (Brannelly *et al.* 2016b), and electrolyte transport and cardiac function
536 (Voyles *et al.* 2009). For example, the SNP *nrf3* (759), is an antioxidant response transcription factor
537 with a protective role in hematopoietic tissues (Chevallard *et al.* 2011); while the SNP, *cab3* (2174), is
538 a regulatory subunit of the voltage-dependent calcium channel that is downregulated in rabbit
539 models with rapid heart rates (Bosch *et al.* 2003). Regulation of calcium channels may impact
540 chytridiomycosis outcomes since *Bd* kills hosts by interfering with electrolyte homeostasis causing
541 eventual cardiac arrest (Voyles *et al.* 2009).

542 **4.6 | IMPLICATIONS FOR THE CAPTIVE BREEDING PROGRAM**

543 Although *P. corroboree* are functionally extinct in the wild, our results suggest that the captive
544 populations (i.e., in terms of allelic richness and heterozygosity) still host good levels of the genetic
545 diversity which may constitute a potential genetic input to wild populations. The immunogenetic
546 variation for *Bd* resistance suggests that genetic manipulation methods could be used to increase
547 species-wide *Bd* resistance to ensure the successful reintroduction of *P. corroboree*. The IUCN's
548 Amphibian Conservation Action Plan recommends establishing captive assurance colonies for
549 amphibians threatened by *Bd* (Gascon *et al.* 2007; Wren *et al.* 2015). In response to these
550 recommendations, the amphibian ARK (AARK) was setup to manage and advise captive breeding
551 efforts, and this successful program currently consists of 188 projects worldwide (AARK database
552 2017). However, because *Bd* cannot be extirpated from the environment, reintroduction projects are
553 unlikely to be effective unless animals with increased resistance are released. The best approaches
554 for increasing disease resistance in captive breeding programs come from livestock and agriculture
555 where they have been successfully applied for over 100 years (Hickey *et al.* 2017). Methods that
556 utilize multiple genetic markers, such as genomic selection, are ideal for increasing disease
557 resistance for wildlife because they have the highest genetic gain (i.e., change in mean trait per year)
558 and the lowest inbreeding rates (Daetwyler *et al.* 2007; Hickey *et al.* 2017; Meuwissen *et al.* 2016).
559 However, before genetic manipulation methods can be applied to corroboree frogs and other
560 species to be released into the wild, several precautions should be undertaken. Most importantly,
561 SNPs used for increasing resistance should be determined from robust, well-powered studies so that
562 conservation managers can be confident of their impact. Additionally, genetically modified animals
563 should be trialed in the field across the range of their environment to ensure that they do not have
564 reduced overall fitness in the wild.

565 **5 | CONCLUDING REMARKS AND FUTURE DIRECTIONS**

566 Southern corroboree frog populations have phenotypic and genetic variation in *Bd* susceptibility.
567 Hence, they have the potential to be genetically manipulated to increase *Bd* resistance. We also

568 show that despite functional extinction in the wild, there is still substantial genetic variation in this
569 species within the captive assurance collection. This pilot study is a first step towards using genomic
570 approaches to investigate polygenic immunity to *Bd*. Future studies should further examine the role
571 that these identified SNPs and MHC variants play in *Bd* resistance. This could be investigated by
572 genetically engineering frogs with gene knock-in approaches or applying genomic selection to
573 increase the frequency of the genes of interest, followed by *Bd*-challenge experiments to measure
574 their impact on the resistance phenotype. Additional studies should also strive to fully characterize
575 the genetic architecture and heritability of *Bd* resistance by performing high resolution QTL
576 association mapping and high-powered GWAS. Lastly, high quality genomic resources for amphibians
577 are required to inform GWAS and comparative genome analyses.

578

579 **ACKNOWLEDGMENTS**

580 We extend sincere thanks to Gerry Marantelli for providing the corroboree frogs used in this study.
581 We are grateful to Collin Storlie, Rhondda Jones, Donald McKnight, and the JCU eResearch team for
582 providing R scripting and statistical assistance, Rebecca Webb, Jennifer Hawkes, Ket Fossen, and
583 Cam De Jong for assistance with animal husbandry, Sara Bell for disease testing assistance, David
584 Hunter for conservation agency support, Michael McFadden, Peter Harlow, and Raelene Hobbs for
585 animal husbandry advice and Kyall Zenger, John Eimes and Arild Husby for discussion of analysis
586 approaches. Funding was provided by the Australian Research Council grants LP110200240 and
587 FT100100375, New South Wales Office of Environment and Heritage, Taronga Zoo, experiment.com
588 crowdfunding grant “Can we stop amphibian extinction by increasing immunity to the frog chytrid
589 fungus”, and Queensland Department of Science, Information Technology and Innovation Accelerate
590 Fellowship grant 14-218.

591 **REFERENCES**

- 592 Adamack, A. T., & Gruber, B. (2014). PopGenReport: simplifying basic population genetic analyses in
593 R. *Methods in Ecology and Evolution*, 5(4), 384-387. doi:10.1111/2041-210X.12158
- 594 Aguilar, J. R.-d., Westerdahl, H., Puente, J. M.-d. I., Tomás, G., Martínez, J., & Merino, S. (2016). MHC-
595 I provides both quantitative resistance and susceptibility to blood parasites in blue tits in the
596 wild. *Journal of Avian Biology*. doi:10.1111/jav.00830
- 597 Alberts, B., Johnson, A., Lewis, J., Walter, P., Raff, M., & Roberts, K. (2002). *Molecular Biology of the*
598 *Cell 4th Edition: International Student Edition*: Routledge.
- 599 Ali, S., Jenkins, Y., Kirkley, M., Dagkalis, A., Manivannan, A., Crane, I. J., & Kirby, J. A. (2008).
600 Leukocyte Extravasation: An immunoregulatory role for α -L Fucosidase? *J Immunol*, 181(4),
601 2407-2413.
- 602 Allendorf, F., Luikart, G., & Aitken, S. (2013). Conservation and the genetics of populations.
- 603 Allendorf, F. W. (1986). Genetic drift and the loss of alleles versus heterozygosity. *Zoo Biol*, 5(2), 181-
604 190.
- 605 Aulchenko, Y. S., Ripke, S., Isaacs, A., & Van Duijn, C. M. (2007). GenABEL: an R library for genome-
606 wide association analysis. *Bioinformatics*, 23(10), 1294-1296.
- 607 Babik, W. (2010). Methods for MHC genotyping in non-model vertebrates. *Mol Ecol Resour*, 10(2),
608 237-251.
- 609 Ballou, J. D., & Lacy, R. C. (1995). Identifying genetically important individuals for management of
610 genetic variation in pedigreed populations. *Population management for survival and*
611 *recovery*, 76-111.
- 612 Bataille, A., Cashins, S. D., Grogan, L., Skerratt, L. F., Hunter, D., McFadden, M., . . . Harlow, P. S.
613 (2015). Susceptibility of amphibians to chytridiomycosis is associated with MHC class II
614 conformation. *Proceedings of the Royal Society of London B: Biological Sciences*, 282.
- 615 Béréños, C., Ellis, P. A., Pilkington, J. G., Lee, S. H., Gratten, J., & Pemberton, J. M. (2015).
616 Heterogeneity of genetic architecture of body size traits in a free-living population. *Mol Ecol*,
617 24(8), 1810-1830. doi:doi: 10.1111/mec.13146
- 618 Berger, L., Speare, R., Daszak, P., Green, D. E., Cunningham, A. A., Goggin, C. L., . . . McDonald, K. R.
619 (1998). Chytridiomycosis causes amphibian mortality associated with population declines in
620 the rain forests of Australia and central America. *Proc Natl Acad Sci*, 95.
621 doi:10.1073/pnas.95.15.9031
- 622 Bosch, R. F., Scherer, C. R., Rüb, N., Wöhr, S., Steinmeyer, K., Haase, H., . . . Kühlkamp, V. (2003).
623 Molecular mechanisms of early electrical remodeling: transcriptional downregulation of ion
624 channel subunits reduces I_{Ca}, I_L and I_T in rapid atrial pacing in rabbits. *Journal of the*
625 *American College of Cardiology*, 41(5), 858-869.
- 626 Boyle, D. G., Boyle, D. B., Olsen, V., Morgan, J. A., & Hyatt, A. D. (2004). Rapid quantitative detection
627 of chytridiomycosis (*Batrachochytrium dendrobatidis*) in amphibian samples using real-time
628 Taqman PCR assay. *Dis Aquat Organ*, 60(2), 141-148. doi:10.3354/dao060141
- 629 Brannelly, L. A., Berger, L., Marrantelli, G., & Skerratt, L. F. (2015a). Low humidity is a failed
630 treatment option for chytridiomycosis in the critically endangered southern corroboree frog.
631 *Wildlife Research*, 42(1), 44-49.
- 632 Brannelly, L. A., Hunter, D. A., Skerratt, L. F., Scheele, B. C., Lenger, D., McFadden, M. S., . . . Berger,
633 L. (2015b). Chytrid infection and post-release fitness in the reintroduction of an endangered
634 alpine tree frog. *Animal Conservation*. doi:10.1111/acv.12230
- 635 Brannelly, L. A., Skerratt, L. F., & Berger, L. (2015c). Treatment trial of clinically ill corroboree frogs
636 with chytridiomycosis with two triazole antifungals and electrolyte therapy. *Veterinary*
637 *Research Communications*, 39(3), 179-187.
- 638 Brannelly, L. A., Webb, R., Skerratt, L. F., & Berger, L. (2016a). Amphibians with infectious disease
639 increase their reproductive effort: evidence for the terminal investment hypothesis. *Open*
640 *Biology*, 6(6). doi:10.1098/rsob.150251

- 641 Brannelly, L. A., Webb, R. J., Skerratt, L. F., & Berger, L. (2016b). Effects of chytridiomycosis on
642 hematopoietic tissue in the spleen, kidney and bone marrow in three diverse amphibian
643 species. *Pathogens and Disease*. doi:10.1093/femspd/ftw069
- 644 Chevillard, G., Paquet, M., & Blank, V. (2011). Nfe2l3 (Nrf3) deficiency predisposes mice to T-cell
645 lymphoblastic lymphoma. *Blood*, 117(6), 2005-2008.
- 646 Clarke, G. M., Anderson, C. A., Pettersson, F. H., Cardon, L. R., Morris, A. P., & Zondervan, K. T.
647 (2011). Basic statistical analysis in genetic case-control studies. *Nat Protoc*, 6(2), 121-133.
648 doi:10.1038/nprot.2010.182
- 649 Cruz, V. M., Kilian, A., & Dierig, D. A. (2013). Development of DArT marker platforms and genetic
650 diversity assessment of the U.S. collection of the new oilseed crop *Lesquerella* and related
651 species. *PLoS One*, 8(5), e64062. doi:10.1371/journal.pone.0064062
- 652 Daetwyler, H. D., Villanueva, B., Bijma, P., & Woolliams, J. A. (2007). Inbreeding in genome-wide
653 selection. *Journal of Animal Breeding and Genetics*, 124(6), 369-376.
- 654 Delport, W., Poon, A. F., Frost, S. D., & Pond, S. L. K. (2010). Datamonkey 2010: a suite of
655 phylogenetic analysis tools for evolutionary biology. *Bioinformatics*, 26(19), 2455-2457.
- 656 Didinger, C., Eimes, J. A., Lillie, M., & Waldman, B. (2017). Multiple major histocompatibility complex
657 class I genes in Asian anurans: Ontogeny and phylogeny of expression. *Developmental &
658 Comparative Immunology*. doi:10.1016/j.dci.2016.12.003
- 659 Do, C., Waples, R. S., Peel, D., Macbeth, G., Tillett, B. J., & Ovenden, J. R. (2014). NeEstimator v2: re-
660 implementation of software for the estimation of contemporary effective population size
661 (Ne) from genetic data. *Mol Ecol Resour*, 14(1), 209-214.
- 662 Doudna, J. A., & Charpentier, E. (2014). The new frontier of genome engineering with CRISPR-Cas9.
663 *Science*, 346(6213). doi:10.1126/science.1258096
- 664 Earl, D. A. (2012). STRUCTURE HARVESTER: a website and program for visualizing STRUCTURE output
665 and implementing the Evanno method. *Conservation Genetics Resources*, 4(2), 359-361.
666 doi:10.1007/s12686-011-9548-7
- 667 Ellison, A. R., Savage, A. E., DiRenzo, G. V., Langhammer, P., Lips, K. R., & Zamudio, K. R. (2014a).
668 Fighting a losing battle: vigorous immune response countered by pathogen suppression of
669 host defenses in the chytridiomycosis-susceptible frog *Atelopus zeteki*. *Genes Genomes
670 Genetics*, 4(7), 1275-1289. doi:10.1534/g3.114.010744
- 671 Ellison, A. R., Tunstall, T., DiRenzo, G. V., Hughey, M. C., Rebollar, E. A., Belden, L. K., . . . Zamudio, K.
672 R. (2014b). More than skin deep: functional genomic basis for resistance to amphibian
673 chytridiomycosis. *Genome Biology and Evolution*, 7(1), 286-298. doi:10.1093/gbe/evu285
- 674 Evanno, G., Regnaut, S., & Goudet, J. (2005). Detecting the number of clusters of individuals using
675 the software STRUCTURE: a simulation study. *Mol Ecol*, 14(8), 2611-2620.
676 doi:10.1111/j.1365-294X.2005.02553.x
- 677 Excoffier, L., & Lischer, H. E. (2010). Arlequin suite ver 3.5: a new series of programs to perform
678 population genetics analyses under Linux and windows. *Mol Ecol Resour*, 10.
679 doi:10.1111/j.1755-0998.2010.02847.x
- 680 Falconer, D. S., Mackay, T. F., & Frankham, R. (1996). Introduction to quantitative genetics (4th edn).
681 *Trends in Genetics*, 12(7), 280.
- 682 Falush, D., Stephens, M., & Pritchard, J. K. (2007). Inference of population structure using multilocus
683 genotype data: dominant markers and null alleles. *Mol Ecol Resour*, 7(4), 574-578.
- 684 Felsenstein, J. (1985). Confidence limits on phylogenies: an approach using the bootstrap. *Evolution*,
685 39(4), 783-791.
- 686 Fernández-Loras, A., Fernández-Beaskoetxea, S., Arriero, E., Fisher, M. C., & Bosch, J. (2017). Early
687 exposure to *Batrachochytrium dendrobatidis* causes profound immunosuppression in
688 amphibians. *European Journal of Wildlife Research*, 63(6), 99. doi:10.1007/s10344-017-
689 1161-y

- 690 Fites, J. S., Ramsey, J. P., Holden, W. M., Collier, S. P., Sutherland, D. M., Reinert, L. K., . . . Rollins-
691 Smith, L. A. (2013). The invasive chytrid fungus of amphibians paralyzes lymphocyte
692 responses. *Science*, 342(6156), 366-369. doi:10.1126/science.1243316
- 693 Galan, M., Guivier, E., Caraux, G., Charbonnel, N., & Cosson, J.-F. (2010). A 454 multiplex sequencing
694 method for rapid and reliable genotyping of highly polymorphic genes in large-scale studies.
695 *BMC genomics*, 11(1), 296. doi:10.1186/1471-2164-11-296
- 696 Garner, T. W. J., Schmidt, B. R., Martel, A., Pasmans, F., Muths, E., Cunningham, A. A., . . . Bosch, J.
697 (2016). Mitigating amphibian chytridiomycoses in nature. *Philosophical Transactions of the*
698 *Royal Society B: Biological Sciences*, 371(1709). doi:10.1098/rstb.2016.0207
- 699 Gascon, C., Collins, J., Moore, R., Church, D., McKay, J., & Mendelson III, J. (2007). Amphibian
700 Conservation Action Plan: The World Conservation Union (IUCN), Gland, Switzerland.
- 701 Götz, S., García-Gómez, J. M., Terol, J., Williams, T. D., Nagaraj, S. H., Nueda, M. J., . . . Conesa, A.
702 (2008). High-throughput functional annotation and data mining with the Blast2GO suite.
703 *Nucleic acids research*, 36(10), 3420-3435.
- 704 Harrison, K. A., Pavlova, A., Telonis-Scott, M., & Sunnucks, P. (2014). Using genomics to characterize
705 evolutionary potential for conservation of wild populations. *Evolutionary Applications*, 7(9),
706 1008-1025.
- 707 Hayes, B., Bowman, P., Chamberlain, A., & Goddard, M. (2009). Invited review: Genomic selection in
708 dairy cattle: Progress and challenges. *Journal of dairy science*, 92(2), 433-443.
- 709 Hebard, F. V. (2006). The backcross breeding program of the American chestnut foundation. *Journal*
710 *of the American Chestnut Foundation*, 19, 55-77.
- 711 Hickey, J. M., Chiurugwi, T., Mackay, I., Powell, W., & Implementing Genomic Selection in, C. B. P. W.
712 P. (2017). Genomic prediction unifies animal and plant breeding programs to form platforms
713 for biological discovery. *Nat Genet*, 49(9), 1297-1303. doi:10.1038/ng.3920
- 714 Hudson, M. A., Young, R. P., Lopez, J., Martin, L., Fenton, C., McCrea, R., . . . Cunningham, A. A.
715 (2016). In-situ itraconazole treatment improves survival rate during an amphibian
716 chytridiomycosis epidemic. *Biological Conservation*, 195, 37-45.
717 doi:http://dx.doi.org/10.1016/j.biocon.2015.12.041
- 718 Hunter, D. (2012). National Recovery Plan for the Southern Corroboree Frog *Pseudophryne*
719 *corroboree* and Northern Corroboree Frog *Pseudophryne pengilleyi*. Office of Environment
720 and Heritage (NSW), Hurstville.
- 721 Hunter, D., Marantelli, G., McFadden, M., Harlow, P., Scheele, B., & Pietsch, R. (2010a). Assessment
722 of re-introduction methods for the southern corroboree frog in the Snowy Mountains region
723 of Australia. *Global re-introduction perspectives: additional case-studies from around the*
724 *globe*. IUCN/SSC Reintroduction Specialist Group, Abu Dhabi, 72-76.
- 725 Hunter, D., Pietsch, R., Marantelli, G., McFadden, M., & Harlow, P. (2009). Field research, recovery
726 actions, and recommendations for the southern corroboree frog (*Pseudophryne corroboree*)
727 recovery program: 2007-2009. Murray Catchment Management Authority.
- 728 Hunter, D. A. (2000). *The conservation and demography of the southern corroboree frog*
729 (*Pseudophryne corroboree*). Master's thesis, University of Canberra.
- 730 Hunter, D. A., Speare, R., Marantelli, G., Mendez, D., Pietsch, R., & Osborne, W. (2010b). Presence of
731 the amphibian chytrid fungus *Batrachochytrium dendrobatidis* in threatened corroboree frog
732 populations in the Australian Alps. *Dis Aquat Organ*, 92(2-3), 209-216.
- 733 International H. I. V. Controllers Study, T., Writing, t., Pereyra, F., Jia, X., McLaren, P. J., Telenti, A., . .
734 . Zhao, M. (2010). The Major Genetic Determinants of HIV-1 Control Affect HLA Class I
735 Peptide Presentation. *Science*, 330(6010), 1551-1557. doi:10.1126/science.1195271
- 736 James, T. Y., Toledo, L. F., Rödder, D., da Silva Leite, D., Belasen, A. M., Betancourt-Román, C. M., . . .
737 Longcore, J. E. (2015). Disentangling host, pathogen, and environmental determinants of a
738 recently emerged wildlife disease: lessons from the first 15 years of amphibian
739 chytridiomycosis research. *Ecology and Evolution*. doi:10.1002/ece3.1672

- 740 Jannink, J.-L., Lorenz, A. J., & Iwata, H. (2010). Genomic selection in plant breeding: from theory to
741 practice. *Briefings in functional genomics*, 9(2), 166-177.
- 742 Jombart, T., Devillard, S., & Balloux, F. (2010). Discriminant analysis of principal components: a new
743 method for the analysis of genetically structured populations. *BMC genetics*, 11(1), 1.
- 744 Judo, M. S., Wedel, A. B., & Wilson, C. (1998). Stimulation and suppression of PCR-mediated
745 recombination. *Nucleic acids research*, 26(7), 1819-1825.
- 746 Keenan, K., McGinnity, P., Cross, T. F., Crozier, W. W., & Prodöhl, P. A. (2013). *diveRsity*: An R
747 package for the estimation and exploration of population genetics parameters and their
748 associated errors. *Methods in Ecology and Evolution*, 4(8), 782-788. doi:10.1111/2041-
749 210X.12067
- 750 Kiemnec-Tyburczy, K., Richmond, J., Savage, A., Lips, K., & Zamudio, K. (2012). Genetic diversity of
751 MHC class I loci in six non-model frogs is shaped by positive selection and gene duplication.
752 *Heredity*, 109(3), 146-155.
- 753 Klein, J., Bontrop, R. E., Dawkins, R. L., Erlich, H. A., Gyllensten, U. B., Heise, E. R., . . . Watkins, D. I.
754 (1993). Nomenclature for the major histocompatibility complexes of different species: a
755 proposal *The HLA System in Clinical Transplantation* (pp. 407-411): Springer.
- 756 Kliman, R., Sheehy, B., & Schultz, J. (2008). Genetic drift and effective population size. *Nature*
757 *Education*, 1(3), 3.
- 758 Koch, M., Camp, S., Collen, T., Avila, D., Salomonsen, J., Wallny, H.-J., . . . Kaufman, J. (2007).
759 Structures of an MHC Class I Molecule from B21 Chickens Illustrate Promiscuous Peptide
760 Binding. *Immunity*, 27(6), 885-899. doi:https://doi.org/10.1016/j.immuni.2007.11.007
- 761 Kosakovsky Pond, S. L., Posada, D., Gravenor, M. B., Woelk, C. H., & Frost, S. D. (2006). Automated
762 phylogenetic detection of recombination using a genetic algorithm. *Mol Biol Evol*, 23(10),
763 1891-1901. doi:10.1093/molbev/msl051
- 764 Kosch, T. A., Eimes, J. A., Didingler, C., Brannelly, L. A., Waldman, B., Berger, L., & Skerratt, L. F.
765 (2017). Characterization of MHC class IA in the endangered southern corroboree frog.
766 *Immunogenetics*, 69(3), 165-174. doi:10.1007/s00251-016-0965-3
- 767 Kriger, K. M., Hero, J.-M., & Ashton, K. J. (2006). Cost efficiency in the detection of chytridiomycosis
768 using PCR assay. *Dis Aquat Organ*, 71(2), 149-154.
- 769 Kumar, S., Stecher, G., & Tamura, K. (2016). MEGA7: Molecular Evolutionary Genetics Analysis
770 Version 7.0 for Bigger Datasets. *Molecular biology and evolution*, 33(7), 1870-1874.
771 doi:10.1093/molbev/msw054
- 772 Lau, Q., Igawa, T., Komaki, S., & Satta, Y. (2016). Characterisation of major histocompatibility
773 complex class I genes in Japanese Ranidae frogs. *Immunogenetics*, 1-10.
- 774 Lebrón, J. A., Bennett, M. J., Vaughn, D. E., Chirino, A. J., Snow, P. M., Mintier, G. A., . . . Bjorkman, P.
775 J. (1998). Crystal Structure of the Hemochromatosis Protein HFE and Characterization of Its
776 Interaction with Transferrin Receptor. *Cell*, 93(1), 111-123. doi:10.1016/S0092-
777 8674(00)81151-4
- 778 Lees, C., McFadden, M., & Hunter, D. (2013). Genetic Management of Southern Corroboree Frogs:
779 Workshop Report and Plan. IUCN Conservation Breeding Specialist Group, Apple Valley, MN.
- 780 Lewontin, R., & Krakauer, J. (1973). Distribution of gene frequency as a test of the theory of the
781 selective neutrality of polymorphisms. *Genetics*, 74(1), 175-195.
- 782 Lipovich, L., Lynch, E. D., Lee, M. K., & King, M. C. (2001). A novel sodium bicarbonate cotransporter-
783 like gene in an ancient duplicated region: SLC4A9 at 5q31. *Genome Biol*, 2(4), Research0011.
- 784 Luu, K., Bazin, E., & Blum, M. G. (2017). *pcadapt*: an R package to perform genome scans for
785 selection based on principal component analysis. *Mol Ecol Resour*, 17(1), 67-77.
786 doi:10.1111/1755-0998.12592
- 787 Madsen, T., & Ujvari, B. (2006). MHC class I variation associates with parasite resistance and
788 longevity in tropical pythons. *J Evol Biol*, 19(6), 1973-1978. doi:10.1111/j.1420-
789 9101.2006.01158.x

- 790 Maeshima, K., Morimatsu, K., & Horii, T. (1996). Purification and characterization of XRad51. 1
791 protein, *Xenopus* RAD51 homologue: recombinant XRad51. 1 promotes strand exchange
792 reaction. *Genes to Cells*, 1(12), 1057-1068.
- 793 Maher, B. (2008). Personal genomes: The case of the missing heritability. *Nature News*, 456(7218),
794 18-21.
- 795 Matsumura, M., Fremont, D. H., Peterson, P. A., & Wilson, I. A. (1992). Emerging principles for the
796 recognition of peptide antigens by MHC class I molecules. *Science*, 257(5072), 927-934.
- 797 McFadden, M., Hobbs, R., Marantelli, G., Harlow, P., Banks, C., & Hunter, D. (2013). Captive
798 management and breeding of the critically endangered southern corroboree frog
799 (*Pseudophryne corroboree*)(Moore 1953) at Taronga and Melbourne Zoos. *Amphibian and*
800 *Reptile Conservation*, 5(3), 70-87.
- 801 McFadden, M., Hunter, D., Harlow, P., Pietsch, R., & Scheele, B. (2010). Captive management and
802 experimental re-introduction of the Booroolong Frog on the South Western Slopes region,
803 New South Wales, Australia. *Global Re-introduction Perspectives: 2010*, 77.
- 804 Meuwissen, T., Hayes, B., & Goddard, M. (2016). Genomic selection: A paradigm shift in animal
805 breeding. *Animal frontiers*, 6(1), 6-14.
- 806 Morgan, M. J., Hunter, D., Pietsch, R., Osborne, W., & Keogh, J. S. (2008). Assessment of genetic
807 diversity in the critically endangered Australian corroboree frogs, *Pseudophryne corroboree*
808 and *Pseudophryne pengillyei*, identifies four evolutionarily significant units for conservation.
809 *Mol Ecol*, 17(15), 3448-3463.
- 810 Narum, S. R., Buerkle, C. A., Davey, J. W., Miller, M. R., & Hohenlohe, P. A. (2013). Genotyping-by-
811 sequencing in ecological and conservation genomics. *Mol Ecol*, 22(11), 2841-2847.
812 doi:10.1111/mec.12350
- 813 Nei, M., & Gojobori, T. (1986). Simple methods for estimating the numbers of synonymous and
814 nonsynonymous nucleotide substitutions. *Molecular biology and evolution*, 3(5), 418-426.
- 815 Newhouse, A. E., Polin-McGuigan, L. D., Baier, K. A., Valletta, K. E., Rottmann, W. H., Tschaplinski, T.
816 J., . . . Powell, W. A. (2014). Transgenic American chestnuts show enhanced blight resistance
817 and transmit the trait to T1 progeny. *Plant Science*, 228, 88-97.
- 818 Oleksyk, T. K., Smith, M. W., & O'Brien, S. J. (2010). Genome-wide scans for footprints of natural
819 selection. *Philosophical Transactions of the Royal Society of London B: Biological Sciences*,
820 365(1537), 185-205.
- 821 Olson, D. H., Aanensen, D. M., Ronnenberg, K. L., Powell, C. I., Walker, S. F., Bielby, J., . . . Fisher, M.
822 C. (2013). Mapping the global emergence of *Batrachochytrium dendrobatidis*, the amphibian
823 chytrid fungus. *PLoS One*, 8(2), e56802.
- 824 Osborne, W., Hunter, D., & Hollis, G. (1999). Population declines and range contraction in Australian
825 alpine frogs. *Declines and Disappearances of Australian Frogs*, 145-157.
- 826 Petersen, B. (2017). Basics of genome editing technology and its application in livestock species.
827 *Reproduction in Domestic Animals*, 52, 4-13. doi:10.1111/rda.13012
- 828 Petersen, C., Fuzesi, L., & Hoyer-Fender, S. (1999). Outer dense fibre proteins from human sperm
829 tail: molecular cloning and expression analyses of two cDNA transcripts encoding proteins of
830 approximately 70 kDa. *Mol Hum Reprod*, 5(7), 627-635.
- 831 Pinheiro, J., Bates, D., DebRoy, S., Sarkar, D., & Team, R. C. (2009). nlme: Linear and nonlinear mixed
832 effects models. R package version, 3, 96.
- 833 Poorten, T. J., Stice-Kishiyama, M. J., Briggs, C. J., & Rosenblum, E. B. (2016). Mountain Yellow-legged
834 Frogs (*Rana muscosa*) did not Produce Detectable Antibodies in Immunization Experiments
835 with *Batrachochytrium dendrobatidis*. *J Wildl Dis*, 52(1), 154-158. doi:10.7589/2015-06-156
- 836 Pritchard, J. K., Stephens, M., & Donnelly, P. (2000). Inference of population structure using
837 multilocus genotype data. *Genetics*, 155(2), 945-959.
- 838 Ramsey, J. P., Reinert, L. K., Harper, L. K., Woodhams, D. C., & Rollins-Smith, L. A. (2010). Immune
839 defenses against *Batrachochytrium dendrobatidis*, a fungus linked to global amphibian
840 declines, in the South African clawed frog, *Xenopus laevis*. *Infect Immun*, 78(9), 3981-3992.

- 841 Ribas, L., Li, M. S., Doddington, B. J., Robert, J., Seidel, J. A., Kroll, J. S., . . . Fisher, M. C. (2009).
842 Expression profiling the temperature-dependent amphibian response to infection by
843 *Batrachochytrium dendrobatidis* PLoS One, 4(12), e8408.
844 doi:10.1371/journal.pone.0008408
- 845 Rocha, N., & Neefjes, J. (2008). MHC class II molecules on the move for successful antigen
846 presentation. The EMBO journal, 27(1), 1-5. doi:10.1038/sj.emboj.7601945
- 847 Rollins-Smith, L. A., Ramsey, J. P., Reinert, L. K., Woodhams, D. C., Livo, L. J., & Carey, C. (2009).
848 Immune defenses of *Xenopus laevis* against *Batrachochytrium dendrobatidis*
849 Front Biosci (Schol Ed), 1, 68-91.
- 850 Rollins-Smith, L. A., Woodhams, D. C., Reinert, L. K., Vredenburg, V. T., Briggs, C. J., Nielsen, P. F., &
851 Conlon, J. M. (2006). Antimicrobial peptide defenses of the mountain yellow-legged frog
852 (*Rana muscosa*). Dev Comp Immunol, 30(9), 831-842. doi:10.1016/j.dci.2005.10.005
- 853 Rönnegård, L., McFarlane, S. E., Husby, A., Kawakami, T., Ellegren, H., & Qvarnström, A. (2016).
854 Increasing the power of genome wide association studies in natural populations using
855 repeated measures—evaluation and implementation. Methods in Ecology and Evolution,
856 7(7), 792-799. doi:10.1111/2041-210X.12535
- 857 Rousset, F. (2008). genepop'007: a complete re-implementation of the genepop software for
858 windows and Linux. Mol Ecol Resour, 8. doi:10.1111/j.1471-8286.2007.01931.x
- 859 Sandberg, M., Eriksson, L., Jonsson, J., Sjöström, M., & Wold, S. (1998). New chemical descriptors
860 relevant for the design of biologically active peptides. A multivariate characterization of 87
861 amino acids. Journal of medicinal chemistry, 41(14), 2481-2491. doi:10.1021/jm9700575
- 862 Santure, A. W., Poissant, J., De Cauwer, I., Oers, K., Robinson, M. R., Quinn, J. L., . . . Slate, J. (2015).
863 Replicated analysis of the genetic architecture of quantitative traits in two wild great tit
864 populations. Mol Ecol, 24(24), 6148-6162.
- 865 Savage, A. E., & Zamudio, K. R. (2011). MHC genotypes associate with resistance to a frog-killing
866 fungus. Proc Natl Acad Sci U S A, 108(40), 16705-16710.
- 867 Schad, K. (2007). Amphibian Population Management Guidelines. Amphibian Ark Amphibian
868 Population Management Workshop. Amphibian Ark.
- 869 Scheele, B. C., Hunter, D. A., Brannelly, L. A., Skerratt, L. F., & Driscoll, D. A. (2017). Reservoir-host
870 amplification of disease impact in an endangered amphibian. Conservation Biology, 31(3),
871 592-600. doi:10.1111/cobi.12830
- 872 Scheele, B. C., Hunter, D. A., Grogan, L. F., Berger, L., Kolby, J. E., McFadden, M. S., . . . Driscoll, D. A.
873 (2014). Interventions for Reducing Extinction Risk in Chytridiomycosis-Threatened
874 Amphibians. Conservation Biology, 28(5), 1195-1205. doi:DOI: 10.1111/cobi.12322
- 875 Silva, C. N. S., McFarlane, S. E., Hagen, I. J., Ronnegard, L., Billing, A. M., Kvalnes, T., . . . Husby, A.
876 (2017). Insights into the genetic architecture of morphological traits in two passerine bird
877 species. Heredity. doi:10.1038/hdy.2017.29
- 878 Skerratt, L. F., Berger, L., Clemann, N., Hunter, D. A., Marantelli, G., Newell, D. A., . . . West, M.
879 (2016). Priorities for management of chytridiomycosis in Australia: saving frogs from
880 extinction. Wildlife Research. doi:http://dx.doi.org/10.1071/WR15071
- 881 Skerratt, L. F., Mendez, D., McDonald, K. R., Garland, S., Livingstone, J., Berger, L., & Speare, R.
882 (2011). Validation of diagnostic tests in wildlife: the case of chytridiomycosis in wild
883 amphibians. Journal of Herpetology, 45(4), 444-450.
- 884 Takashima, M., Hamamoto, M., & Nakase, T. (2000). Taxonomic significance of fucose in the class
885 Urediniomycetes: distribution of fucose in cell wall and phylogeny of urediniomycetous
886 yeasts. Systematic and applied microbiology, 23(1), 63-70.
- 887 Teacher, A. G. F., Garner, T. W. J., & Nichols, R. A. (2009). Evidence for Directional Selection at a
888 Novel Major Histocompatibility Class I Marker in Wild Common Frogs (*Rana temporaria*)
889 Exposed to a Viral Pathogen (*Ranavirus*). PLoS One, 4(2), e4616.
890 doi:10.1371/journal.pone.0004616

- 891 Therneau, T. M. (2015). A Package for Survival Analysis in S (Version version 2.38). Retrieved from
892 <https://CRAN.R-project.org/package=survival>.
- 893 Therneau, T. M., & Grambsch, P. (2000). *Extending the Cox model*.
- 894 van den Hoorn, T., Paul, P., Jongasma, M. L. M., & Neefjes, J. (2011). Routes to manipulate MHC class
895 II antigen presentation. *Current opinion in immunology*, 23(1), 88-95.
896 doi:<https://doi.org/10.1016/j.coi.2010.11.002>
- 897 Van Prooyen, N., Henderson, C. A., Murray, D. H., & Sil, A. (2016). CD103+ Conventional Dendritic
898 Cells Are Critical for TLR7/9-Dependent Host Defense against *Histoplasma capsulatum*, an
899 Endemic Fungal Pathogen of Humans. *PLoS Pathog*, 12(7), e1005749.
- 900 Visscher, P. M., Wray, N. R., Zhang, Q., Sklar, P., McCarthy, M. I., Brown, M. A., & Yang, J. (2017). 10
901 Years of GWAS Discovery: Biology, Function, and Translation. *The American Journal of*
902 *Human Genetics*, 101(1), 5-22. doi:<https://doi.org/10.1016/j.ajhg.2017.06.005>
- 903 Voyles, J., Young, S., Berger, L., Campbell, C., Voyles, W. F., Dinudom, A., . . . Speare, R. (2009).
904 Pathogenesis of chytridiomycosis, a cause of catastrophic amphibian declines. *Science*,
905 326(5952), 582-585. doi:10.1126/science.1176765
- 906 Warr, G. W., Magor, K. E., & Higgins, D. A. (1995). IgY: clues to the origins of modern antibodies.
907 *Immunology Today*, 16(8), 392-398.
- 908 Whitworth, K. M., Rowland, R. R., Ewen, C. L., Tribble, B. R., Kerrigan, M. A., Cino-Ozuna, A. G., . . .
909 Mileham, A. J. (2016). Gene-edited pigs are protected from porcine reproductive and
910 respiratory syndrome virus. *Nature biotechnology*, 34(1), 20-22.
- 911 Wilson, D. J., & McVean, G. (2006). Estimating diversifying selection and functional constraint in the
912 presence of recombination. *Genetics*, 172. doi:10.1534/genetics.105.044917
- 913 Woodhams, D. C., Bosch, J., Briggs, C. J., Cashins, S., Davis, L. R., Lauer, A., . . . Sheafor, B. (2011).
914 Mitigating amphibian disease: strategies to maintain wild populations and control
915 chytridiomycosis. *Front Zool*, 8(1), 8.
- 916 Wren, S., Angulo, A., Meredith, H. M., Kielgast, J., Dos Santos, M., & Bishop, P. J. (2015). Amphibian
917 Conservation Action Plan. IUCN SSC Amphibian Specialist Group.
- 918 Yamamoto, T., Hikino, T., Nakayama, Y., & Abé, S. I. (1999). Newt RAD51: Cloning of cDNA and
919 analysis of gene expression during spermatogenesis. *Development, growth & differentiation*,
920 41(4), 401-406.
- 921 Yang, J., Benyamin, B., McEvoy, B. P., Gordon, S., Henders, A. K., Nyholt, D. R., . . . Montgomery, G.
922 W. (2010). Common SNPs explain a large proportion of the heritability for human height. *Nat*
923 *Genet*, 42(7), 565-569.
- 924 Young, S., Whitehorn, P., Berger, L., Skerratt, L. F., Speare, R., Garland, S., & Webb, R. (2014). Defects
925 in Host Immune Function in Tree Frogs with Chronic Chytridiomycosis. *PLoS One*.
- 926 Zylstra, P., Rothenfluh, H. S., Weiller, G. F., Blanden, R. V., & Steele, E. J. (1998). PCR amplification of
927 murine immunoglobulin germline V genes: strategies for minimization of recombination
928 artefacts. *Immunology and cell biology*, 76(5), 395-405.

929

930 DATA ACCESSIBILITY

931 MHC class IA DNA sequence data is available on GenBank (acc#'s xx-xx). The data generated from
932 this study is accessible on Dryad xxx.

933 **AUTHOR CONTRIBUTIONS**

934 TAK and CNSS drafted the manuscript. TAK conducted MHC sequencing. TAK and QL conducted MHC
935 analysis. CNSS and TAK performed association and population genetic analyses. LAB performed
936 infection study and *Bd* quantitation. All authors contributed to study design, writing the manuscript,
937 and approved the final version.

938 **SUPPORTING INFORMATION**

939 Additional supporting information may be found in the online version of this article

940 **Table S1** MHC class IA Sanger sequencing information

941 **Table S2** MHC class IA genotypes

942 **Table S3** MHC class IA allele frequencies

943 **Table S4** MHC class IA supertype (ST) frequencies

944 **Table S5** Results of GLS for MHC class IA alleles associated maximum infection load

945 **Table S6** Results of GLS for MHC class IA alleles associated with days survived

946 **Table S7** Results of GLS for MHC class IA superotypes associated with maximum infection load

947 **Table S8** Results of GLS for MHC class IA superotypes associated with days survived

948 **Table S9** Descriptive information on the top 10 SNPs for the GWAS models

949 **Table S10** BLAST results of the top 10 SNPs for the GWAS models

950 **Table S11** BLAST results for SNP population outliers

951 **Figure S1** Body condition by population of frogs from *Bd* treatment group

952 **Figure S2** Comparison of ω across the *P. corroboree* MHC class IA amino acid alignment

953 **Figure S3** Discriminate Analysis of Principal Components (DAPC) of MHC class IA superotypes

954 **Figure S4** Evolutionary relationships of MHC Class IA nucleotide sequences and MHC superotypes

955 **Figure S5** Genetic diversity of MHC class IA in *P. corroboree* populations

956 **Figure S6** Influence of supertype 8 on survival

957 **Figure S7** Manhattan plots with $-\log_{10}$ p-values from the GWAS association

958 **Document S1** The detailed description of the methods

959

960

961

962

963 **TABLES**

964 **TABLE 1** MHC class IA genetic diversity statistics by population. (N) number of individuals, (A_P) total
965 number of alleles per pop, (A_i) number of alleles per individual averaged per population, (D_{NUC}) mean
966 pairwise nucleotide diversity (p-distance), (D_{AA}) mean pairwise amino acid diversity (p-distance), (S_P)
967 total number of supertypes per population, and (S_i) number of supertypes per individual averaged
968 per population. () standard deviation

	Population			
	C	J	M	S
N	20	18	22	16
A_P	17	17	20	14
A_i	5.75 (2.15)	5.72 (1.71)	6.41 (1.94)	4.88 (2.28)
P_A	2	0	2	0
D_{NUC}	0.187 (0.020)	0.169 (0.023)	0.183 (0.018)	0.188 (0.031)
D_{AA}	0.322 (0.038)	0.297 (0.034)	0.301 (0.029)	0.312 (0.038)
S_P	8	7	8	7
S_i	4.650 (1.387)	4.611 (1.420)	5.409 (1.469)	4.500 (1.789)

969

970

971

972

973

974

975

976

977

978

979

980

981

982

983

984

985

986

987 **TABLE 2** Corroboree frog population genetic differentiation (F_{ST} values). (upper graph) MHC class IA
 988 alleles (lower half) and SNPs (upper half), (lower graph) 24 outlier SNPs (lower half) and 3465 neutral
 989 SNPs (upper half). bold ($p < 0.05$), * ($p < 0.01$), and ** ($p < 0.001$).

MHC and SNPs				
	C	J	M	S
C	—	0.125**	0.136**	0.114**
J	0.007	—	0.191**	0.106**
M	0.012**	0.009*	—	0.187**
S	0.011	0.000	0.000	—
Outlier and neutral SNPs				
C	—	0.124**	0.133**	0.113**
J	0.363**	—	0.188**	0.105**
M	0.539**	0.601**	—	0.184**
S	0.308**	0.241**	0.551**	—

990
 991
 992
 993
 994
 995
 996
 997
 998
 999
 1000
 1001
 1002
 1003
 1004
 1005
 1006
 1007
 1008
 1009

1010 **TABLE 3** Single nucleotide polymorphism (SNP) genetic diversity statistics by population. (N) number
1011 of individuals, (N_A) number of SNP alleles, (H_O) heterozygosity observed, (H_E) heterozygosity
1012 expected, (A_R) mean allelic richness, (F_{IS}) inbreeding coefficient, and (N_e) effective population size
1013 with 95% confidence intervals

	Population			
	C	J	M	S
N	20	18	22	16
N_A	6888	6793	6900	6721
H_O	0.388	0.370	0.401	0.361
H_E	0.366	0.339	0.374	0.335
A_R	1.37	1.34	1.38	1.34
F_{IS}	-0.050	-0.073	-0.060	-0.065
N_e	7.9 (7.8-7.9)	23.4 (23.2-23.6)	6.8 (6.8-6.8)	11.4 (11.4-11.5)

1014

1015

1016

1017

1018

1019

1020

1021

1022

1023

1024

1025

1026

1027

1028

1029

1030

1031

1032

1033

1034

1035 **TABLE 4** Putative gene functions of notable SNP loci identified by GWAS and outlier analyses

SNP ID	Gene	Putative function	Method	P-value	References
34	Slc4a9	Sodium bicarbonate solute carrier	GWAS: Max	5.10E ⁻¹³	Lipovich <i>et al.</i> 2001
173	Guanine nucleotide exchange factor	A molecular switch involved in cell differentiation and proliferation	GWAS: Days	9.20E ⁻⁰⁵	Alberts <i>et al.</i> 2002
1894, 1895, and 18 others	Alpha-L-tissue fucosidase	Cleaves fucose containing glycoproteins	GWAS and outliers	--	Takashima <i>et al.</i> 2000
3440	Immunoglobulin Y	Pathogen recognition and control	GWAS: Days	0.002	Warr <i>et al.</i> 1995, Ramsey <i>et al.</i> 2010, Young <i>et al.</i> 2014, Poorten <i>et al.</i> 2016, Fernández-Loras <i>et al.</i> 2017
79	RAD51	Genetic recombination and DNA repair	Outlier	6.42E ⁻¹⁵	Maeshima <i>et al.</i> 1996, Yamamoto <i>et al.</i> 1999
2794	Outer dense fiber of sperm tails 2 L	Maintains the elastic structure of sperm tails	Outlier	3.68E ⁻⁰⁵	Petersen <i>et al.</i> 1999
2603	Toll-like receptor 7	Pathogen recognition and innate immunity activation	Outlier	1.50E ⁻⁰⁵	Van Prooyen <i>et al.</i> 2016
759	Nrf3	Antioxidant response transcription factor	Outlier	4.01E ⁻⁰⁷	Chevillard <i>et al.</i> 2011
2174	Cab3	Regulatory subunit of the voltage-dependent calcium channel	Outlier	1.36E ⁻⁰⁵	Bosch <i>et al.</i> 2003, Voyles <i>et al.</i> 2009
928	ORP1 (OSBPL1A)	Multiple functions, including antigen processing and presentation	GWAS: Days	6.80E ⁻⁰⁴	Rocha <i>et al.</i> 2008, van den Hoorn <i>et al.</i> 2011 (van den Hoorn <i>et al.</i> 2011)

1036

1037

1038

1039

1040

1041

1042

1043

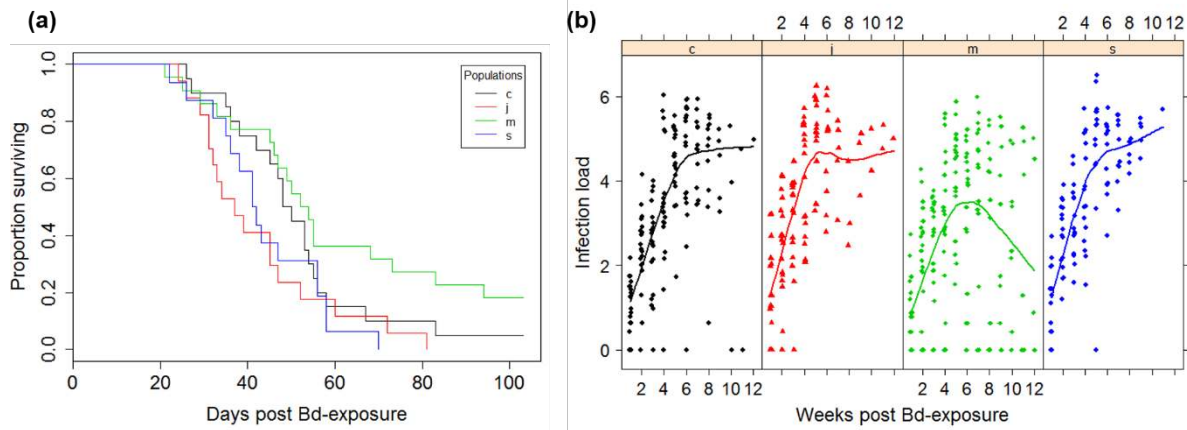
1044

1045

1046

1047

1048 **FIGURES**



1049

1050 **FIGURE 1** Interpopulation variation in *Bd* infection load and mortality in laboratory exposed *P.*
1051 *corroboree*. (a) Daily survivorship in *Bd* infected frogs. (b) *Bd* infection load ($\log_{10}(ZE+1)$) over the
1052 course of the experiment as estimated by qPCR. Trend lines represent smooth fitted population
1053 means. In the second half of the experiment infection load trends for population M diverged from
1054 the other populations as highly infected frogs died, and the means became more influenced by
1055 survivor loads. Populations are represented by (c) Cool Plains, (j) Jagumba, (m) Manjar, and (s)
1056 Snakey Plains

1057

1058

1059

1060

1061

1062

1063

1064

1065

1066

1067

1068

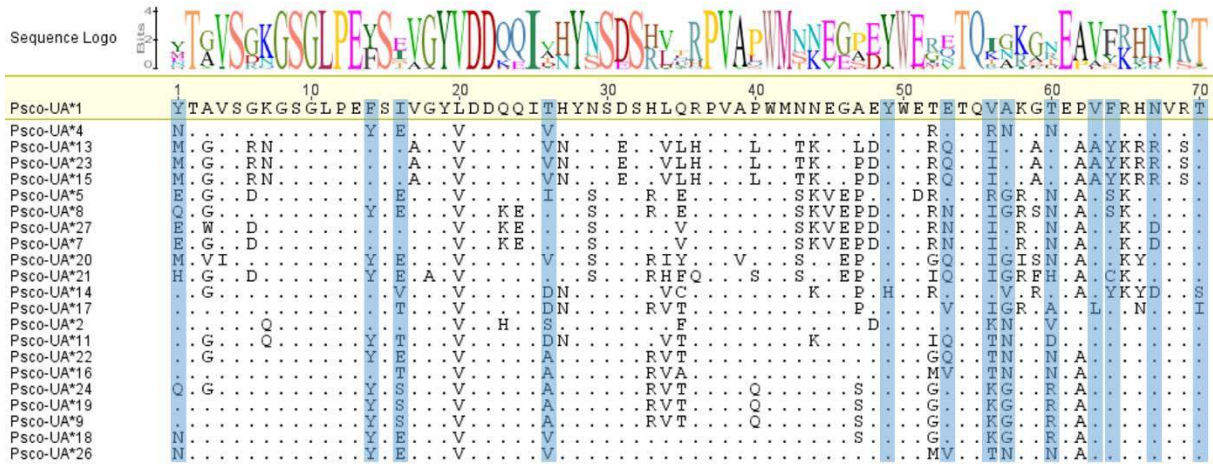
1069

1070

1071

1072

1073



1074

1075 **FIGURE 2** Alignment of *P. corroboree* MHC Class IA amino acid sequences. Peptide binding pocket
 1076 positions from *H. sapiens* (Lebron 1998 and Matsumura 1992) are highlighted in grey. Dots indicate
 1077 homology to the reference sequence Psc0-UA*1

1078

1079

1080

1081

1082

1083

1084

1085

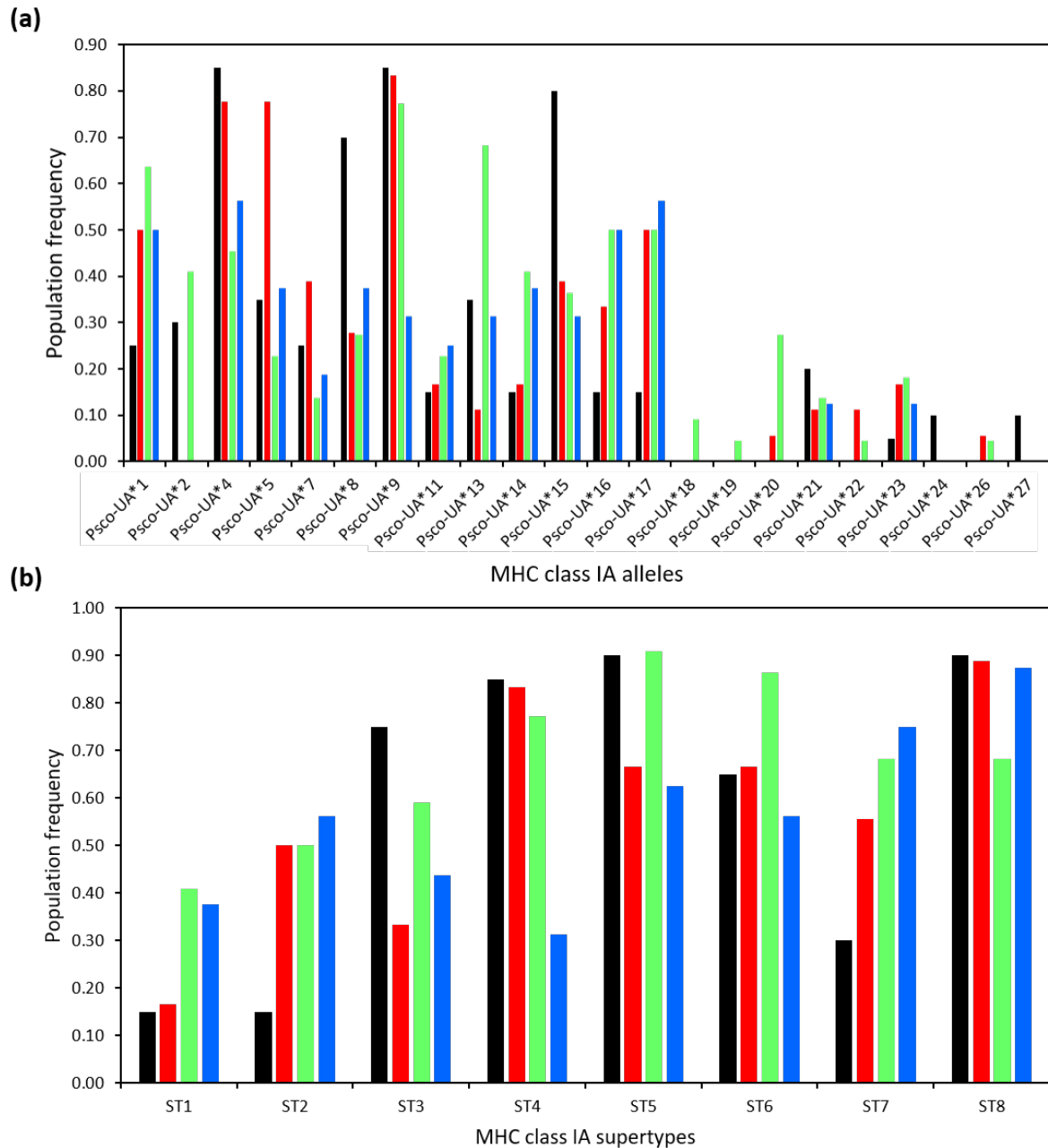
1086

1087

1088

1089

1090



1091

1092 **FIGURE 3** MHC class IA allele and supertype distributions among *P. corroboree* populations. (a) allele
 1093 and (b) supertype (ST) frequency distribution. The incidence of *Bd* susceptibility-associated allele
 1094 (PscO-UA*5) and supertype (ST8) was lowest in population M. (black) population C, (red) population
 1095 J, (green) population M, and (blue) population S

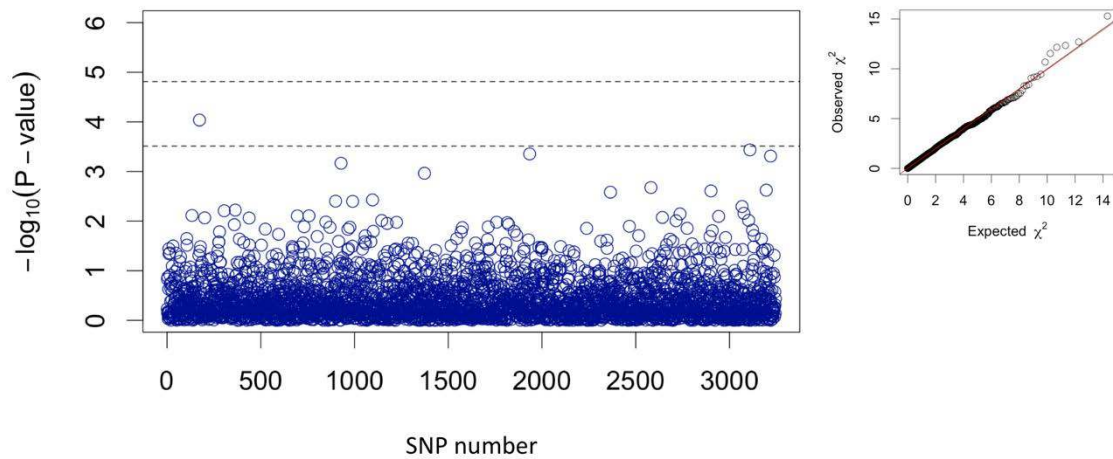
1096

1097

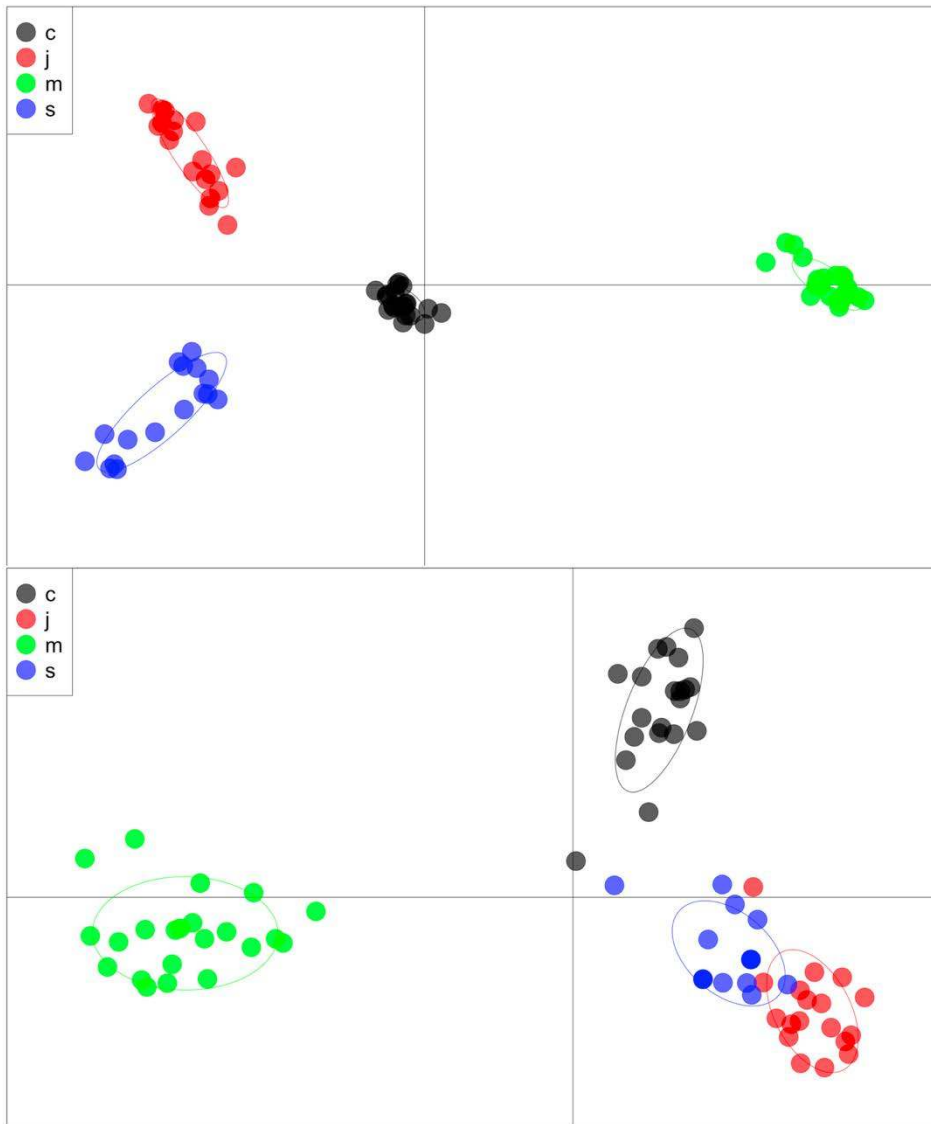
1098

1099

1100



1101
1102 **FIGURE 4** Manhattan plot with $-\log_{10}$ p-values from the association with marker genotype (SNPs) for
1103 days survived using GenABEL. The upper dashed line indicates the genome-wide Bonferroni-
1104 corrected significant threshold and the lower dashed line indicates the suggestive threshold. The
1105 QQ-plot (on the right) shows the relationship between the expected and observed distributions of
1106 SNP level test statistics



1107

1108 **FIGURE 5** Discriminate Analysis of Principal Components (DAPC) using 3465 neutral SNPs (upper
1109 image) and 24 outliers SNPs (lower image). The first 4 PCs explained 29.8% of the variance (a-score =
1110 0.621) when using neutral SNPs (upper image) and the first 5 PCs explained 82.8% of the variance (a-
1111 score = 0.594) when using outlier SNPs (lower image)